UNIVERSIDADE FEDERAL DE MINAS GERAIS
Intituto de Ciências Exatas
Programa de Pós-graduação em Física

Leonardo Santos Lopes

VICSEK MODEL WITH MALTHUSIAN POPULATION DYNAMICS

Belo Horizonte
2021

Leonardo Santos Lopes

VICSEK MODEL WITH MALTHUSIAN POPULATION DYNAMICS

Dissertation submitted to the Physics Graduate Program of Instituto de Ciências Exatas, Universidade Federal de Minas Gerais, in partial fulfillment of the requirements for the degree of Master in Sciences.

Supervisor: Ronald Dickman

Belo Horizonte
2021

Dados Internacionais de Catalogação na Publicação (CIP)

L864v Lopes, Leonardo Santos.
Vicsek model with malthusian population dynamics / Leonardo Santos Lopes. – 2021.
62 f. : il.

Orientador: Ronald Dickman.
Dissertação (mestrado) – Universidade Federal de Minas Gerais, Departamento de Física.
Bibliografia: f. 48-49.

1. Dinâmica populacional. 2. Modelos matemáticos. 3. Malthusianismo. I. Título. II. Dickman, Ronald. III. Universidade Federal de Minas Gerais, Departamento de Física.

CDU – 519.2 (043)

Ficha catalográfica elaborada por Romário Martins Ribeiro – CRB6 3595
Biblioteca Professor Manoel Lopes de Siqueira – Departamento de Física - UFMG

UNIVERSIDADE FEDERAL DE MINAS GERAIS
INSTITUTO DE CIÊNCIAS EXATAS
PROGRAMA DE PÓS-GRADUAÇÃO EM FÍSICA

ATA DE DEFESA DE DISSERTAÇÃO

ATA DA SESSÃO DE ARGUIÇÃO DA 666ª DISSERTAÇÃO DO PROGRAMA DE PÓS-GRADUAÇÃO EM FÍSICA, DEFENDIDA POR LEONARDO SANTOS LOPES, orientado pelo professor Ronald Dickman, para obtenção do grau de **MESTRE EM FÍSICA**. Às 9 horas de cinco de novembro de 2021, por videoconferência, reuniu-se a Comissão Examinadora, composta pelos professores **Ronald Dickman** (Orientador - Departamento de Física/UFMG), **Lucas Lages Wardil** (Departamento de Física/UFMG) e **Hugues Chaté** (CEA/Saclay) para dar cumprimento ao Artigo 37 do Regimento Geral da UFMG, submetendo o bacharel **LEONARDO SANTOS LOPES** à arguição de seu trabalho de dissertação, que recebeu o título de **"Vicsek model with Malthusian dynamics".** O candidato fez uma exposição oral de seu trabalho durante aproximadamente 50 minutos. Após esta, os membros da comissão prosseguiram com a sua arguição e apresentaram seus pareceres individuais sobre o trabalho, concluindo pela aprovação do candidato.

Belo Horizonte, 05 de novembro de 2021.

Prof. Ronald Dickman
Orientador do estudante
Departamento de Física/UFMG

Prof. Lucas Lages Wardil
Departamento de Física/UFMG

Prof. Hugues Chaté
CEA/Saclay

Candidato: Leonardo Santos Lopes

Documento assinado eletronicamente por **Lucas Lages Wardil**, **Professor do Magistério Superior**, em 05/11/2021, às 12:43, conforme horário oficial de Brasília, com fundamento no art. 5º do Decreto nº 10.543, de 13 de novembro de 2020.

Documento assinado eletronicamente por **Ronald Dickman**, **Professor do Magistério Superior**, em 05/11/2021, às 14:34, conforme horário oficial de Brasília, com fundamento no art. 5º do Decreto nº 10.543, de 13 de novembro de 2020.

Documento assinado eletronicamente por **Leonardo Santos Lopes**, **Usuário Externo**, em 10/11/2021, às 15:07, conforme horário oficial de Brasília, com fundamento no art. 5º do Decreto nº 10.543, de 13 de novembro de 2020.

Documento assinado eletronicamente por **Leonardo Santos Lopes**, **Usuário Externo**, em 11/11/2021, às 14:27, conforme horário oficial de Brasília, com fundamento no art. 5º do Decreto nº 10.543, de 13 de novembro de 2020.

Documento assinado eletronicamente por **Hugues Chaté**, **Usuário Externo**, em 26/11/2021, às 14:34, conforme horário oficial de Brasília, com fundamento no art. 5º do Decreto nº 10.543, de 13 de novembro de 2020.

A autenticidade deste documento pode ser conferida no site https://sei.ufmg.br/sei/controlador_externo.php?acao=documento_conferir&id_orgao_acesso_externo=0, informando o código verificador **1061211** e o código CRC **4ECA0CA1**.

Referência: Processo nº 23072.257233/2021-77 SEI nº 1061211

ACKNOWLEDGEMENTS

I would like to thank my supervisor, Ronald Dickman, by his dedication, professionalism and patience. I also acknowledge my family and friends, in special my girlfriend Maria Victoria. I am grateful to the Professor Gerald Weber for his dedication and efforts in keeping our cluster working. I also thanks the Professor Hughes Chaté, for always being helpful, for his suggestions and discussion about my results. The last, but not at least, I am grateful to CAPES and to all the Brazilian people who, amidst the suffering of the pandemic, contributed to this work with their taxes.

RESUMO

A matéria ativa é o ramo da física que estuda sistemas nos quais os indivíduos são autopropelidos, ou seja, não dependem de um agente externo para se movimentar. Alguns exemplos são bandos de pássaros e cardumes de peixes. Nos últimos anos, muita atenção tem sido dada a esse assunto.

O modelo de Vicsek [Vicsek et al.,Phys.Rev.Lett.75,1226] foi o primeiro e o mais simples modelo para explicar o movimento coletivo e a formação de rebanhos usando a perspectiva de transição de fase. Este modelo recebeu muita atenção e demonstrou apresentar quebra de simetria, desenvolvendo ordenamento de longo alcance, mesmo com apenas interações de curto alcance [Toner e Tu, Phys. Rev. E 86, 031918].

Embora o modelo de Vicsek tenha sido extensivamente estudado ao longo dos anos [Ginelli, Eur. Phys. J. Spec. Top. 225, 2099–2117], uma análise teórica mostrou que seria de interesse relaxar a conservação do número de indivíduos [Toner, Phys. Rev. Lett. 108(8):088102]. Além de seu interesse teórico, existem experimentos em que o número de indivíduos não é conservado, incluindo colônias de bactérias e outros sistemas nos quais os indivíduos são criados e destruídos à medida que se movem.

Neste trabalho estudamos um sistema com dinâmica populacional malthusiana (ou seja, a probabilidade de uma partícula morrer é proporcional à densidade na vizinhança da partícula) por meio de métodos computacionais, buscando entender como a densidade estacionária do sistema interage com a intensidade do ruído, como a formação de grupos interfere no número de indivíduos vivos, pois a aplicação do ruído interfere nas propriedades do sistema. Além disso, procuramos classificar a transição de fase e dizer se o sistema apresenta bandas.

Palavras-chave: Malthusiana, Dinâmica populacional, modelo de Vicsek

ABSTRACT

Active matter is the branch of physics that studies systems of interacting self-propelled individuals. Some examples are a bird flocks and schools of fish. In the last few years much attention has been paid to this subject. The Vicsek model [Vicsek et al., Phys. Rev. Lett. **75**, 1226(1995)] was the first and the simplest model to explain the collective movement and formation of herds using the phase transition perspective. This model has been shown to exhibit symmetry breaking, developing long-range order, even with only short-range interactions [Toner, Phys. Rev. E 86, 031918].

While the Vicsek model has been extensively studied over the years [Ginelli, Eur. Phys. J. Spec. Top. **225**, 2099 (2016)], a theoretical analysis has shown that it would be of interest to relax the conservation of the number of individuals [Toner, Phys. Rev. Lett. 108, 088102 (2011)]. In addition to its theoretical interest, there are experiments in which the number of individuals is not conserved, including colonies of bacteria and other systems in which individuals are created and destroyed as they move.

In this work we study a system of active particles with Malthusian population dynamics, that is, the probability of a particle dying is proportional to local particle density. Using simulations, we seek to understand the relation between the stationary density and the noise intensity, how the formation of groups affects population size. Of prime interest is characterizing the phase diagram and determining whether the system exhibits banding.

Keywords: Active matter, Vicsek model, Population dynamics, Malthusian flocks.

CONTENTS

1 Introduction

In many biological systems, individuals form a coherent group that is characterized by cooperative movements. This cooperation arises in various types of systems such as a flock of birds, schools of fish or a colony of bacteria. This cooperative motion can be quite advantageous, either to keep away predators or to be able to carry food [3], so it has been greatly improved by evolution and is studied by many biologists.

Another feature of these groups is the formation of patterns, such as schools of fish that move in circles, shown in Fig.1a. Many of these coordinated motions arise without a leader, via interactions between individuals.

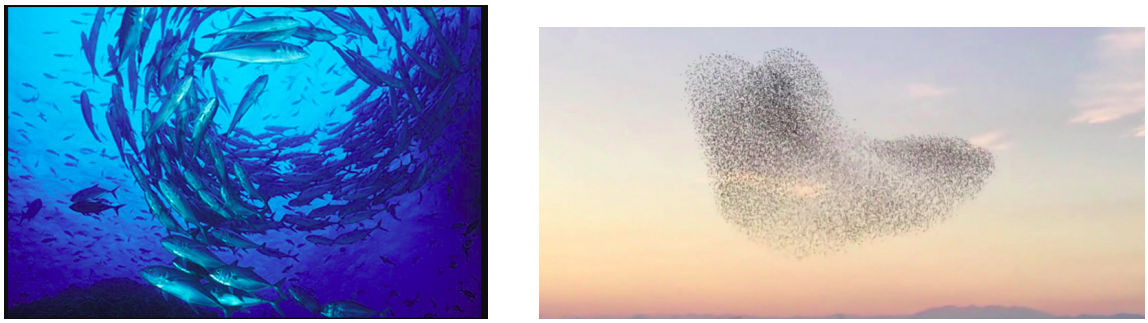

(a) (b)

Figure 1 – Patterns formed by moving groups: (a) A circulating school of fish (b) flock of birds.

It is a challenge for biologists, physicists and computer scientists to understand and model how the orderly movement of these clusters arises and is maintained in such a way as to reproduce the patterns seen in nature. This type of system has been studied for over twenty years and these patterns have only begun to be modeled using self-propelled agents, that is, agents that do not need an external force to move.

The simplest model to study this type of motion is the Vicsek model [17] published in 1995. Vicsek and collaborators addressed the problem from the perspective of phase transitions, in which the system passed from an ordered phase, in which the particles move in coordinated groups, a disordered phase with individuals moving in a uncoordinated manner. In this model, particles move with a constant speed on a 2D surface. Particle interactions are short-ranged, and at each time step the particles tend to align their velocities with their neighbors subject to a random contribution (a noise).

Vicsek model and its variations are used extensively to explain numerous effects in group motion. A good example is the study of vortex motion in schools of fish (Fig.1a),

which was modeled by Constanzo and Hemelrijk [2] using a simple modification of the Vicsek model.

Vicsek and collaborators realized, using numerical simulations, that the model goes from a disordered phase to an ordered phase as the noise decreases. Furthermore, the authors concluded that the transition is continuous and estimated certain critical exponents. These conclusions were challenged in 2004, when Gregoiré and Chaté [5] published a detailed study of the Vicsek model. These authors found that the phase transition is discontinuous; they asserted that Vicsek and collaborators didn't realize this because the original studies employed small systems, making the transition appears continuous.

Chaté and Gregoiré [5] observed the existence of a third phase characterized by one or more dense ordered bands travelling through a disordered dilute region. The transition to collective motion can be interpreted as a liquid-vapor transition. From this point of view, bands corresponds to coexistence of the ordered and disordered phases.

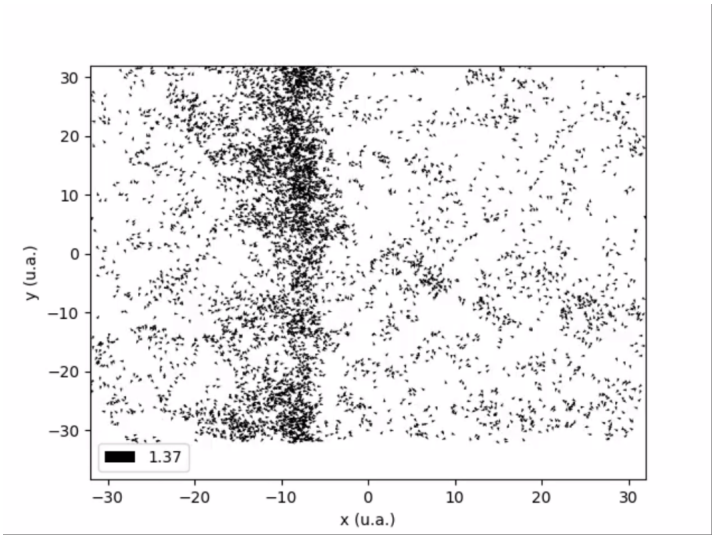

Figure 2 – Vicsek model: Snapshot showing an ordered band passing through a disordered, low-density region.(Unless otherwise stated, all data and images were generated by the author.)

However, all these studies have a constant number of individuals, so that global density, is a fixed intensive parameter. Toner [13] studied continuous models with population conservation using a hydrodynamic description, and concluded that it was not possible to determine exactly the scaling exponents using in their stability analysis of the ordered phase[1]. Nevertheless, in 2011 John Toner [12] argued that it would be advantageous from a theoretical point of view to give up this requirement and investigated a model with a fluctuation population size associated with Malthusian population dynamics. The main

[1] In equilibrium such a phase cannot exist in 2D as stated by Mermim-Wagner theorem [10]. Toner and Tu wanted to show that out of equilibrium, the hydrodynamic description contains nonlinear terms that stabilize the ordered phase

theoretical advantage of this model is that one can determine the scaling exponents exacly in this case.

In addition to the theoretical interest of active matter with population dynamics, there are real systems that do not conserve the number of individuals [9]; a good example is bacterial colonies. Other types of active systems without conservation of individuals are cytoskeletons such as the one studied by Kruse and coworkers [7]. Therefore, it would be interesting to develop a computational study focused on the Malthusian model, mainly addressing its phase diagram and determing the nature of the phase transition. In this work I develop a theoretical model and a simulation code that allows a detailed study of active matter subject to population dynamics.

In Chapter 2 I define Vicsek's model in detail. I weview the conclusions drawn by Vicsek and coworkers [17] and describe the phase transition found by these researchers. Subsequently, I discuss the modifications proposed by Gregoiré and Chaté [5] and their conclusions regarding the Vicsek model, including the emergence of bands and how it changes the understanding of the problem.

In chapter 3 I discuss models with population dynamics reviewing the hydrodynamic analysis by Toner [12], followed by our construction of the theoretical used in simulations.

After that, in chapter 4 I describe the computational methods used in this project, briefly introducing Monte Carlo simulations, the language used, and the random number generator, among other technical issues.

In chapter 5 I present the results obtained, detailing the phase transition and the role of bands. Finally, in chapter 6 contains a brief conclusion and a discussion of directions for future research.

2 The Vicsek Model

2.1 Introduction

The motion of herds or even human crowds [6] has long been of interest to diverse areas of science. For physicists, the greatest interest lies in how the interactions between the agents occur, and how it is possible to have coherent motion without a leader.

The Vicsek model (VM) of self-propelled particles was introduced in efforts to understand how coherent motion arises, from the perspective of phase transitions. Each particle tends to align its velocity with that of its neighbors subject to a random perturbation. This leads to an ordered phase, breaking the rotational symmetry for low noise intensity.

In section 2.2 we introduce the VM and its properties based on the article of Vicsek et al. [17] while in section 2.3 we discuss the modifications proposed by Grégoire and Chaté [5] and the new conclusions their analysis led to.

2.2 Vicsek Model (1995)

2.2.1 Definitions

In order to understand how collective motion of self-propelled organisms occurs in nature, Vicsek and coworkers [17] proposed a model in which each particle moves individually, but an alignment mechanism leads to the emergence of collective motion, very similar to that observed in nature.

A feature of this model is that each particle, with constant speed v_0, assumes the mean direction of motion of the particles in its neighborhood subject to a random perturbation, or *noise*. The noise can be interpreted as a random error affecting each organism's control of their direction, due to limitations in their nervous system or motor control and/or external perturbations (wind, turbulence, etc).

The model is defined as follows: N point particles are restricted to the square $[0, L) \times [0, L)$ with periodic boundaries. Each particle is characterized by a position vector $\mathbf{x}_j$ and direction of motion θ_j; the velocity of particle j is $\mathbf{v}_j = (v_0 \cos\theta_j, v_0 \sin\theta_j)$, with constant speed v_0. The positions and directions evolve in discrete time, at fixed intervals Δt. At each time step the j-th particle takes the position:

$$\mathbf{x}_j(t + \Delta t) = \mathbf{x}_j(t) + \mathbf{v}_j \Delta t, \tag{2.1}$$

and updates its direction θ_j as the average of the angles of the particles in its neighborhood (including itself). The neighborhood of the j-th particle is defined as every individual with a distance less than or equal R_0 of particle j, thus:

$$\theta_j(t+1) = \arg[\sum_{k\sim i} e^{i\theta_k(t)}] + \eta\xi_j(t), \tag{2.2}$$

where the sum is over all particles in the neighborhood of the particle j; The $\xi_j(t)$ are a set of random variables uniformly distributed on $[-\pi, \pi]$ with $< e^{i\xi_k(t)}e^{-i\xi_j(t')} >= \delta_{kj}\delta_{tt'}$ and η is the noise intensity.

Note that noise is added to the mean direction of the neighborhood. The interpretation of this type of noise, known in literature as angular noise (AN), is that the particle accurately calculates the mean direction of its neighbors, but cannot align itself precisely with this direction. We can, without loss of generality, fix $\Delta t = 1$ and $R_0 = 1$ and thus are left with three parameters: η, ρ and v_0, where $\rho = \frac{N}{L^2}$ is the density. We define as initial conditions the following: At time $t = 0$, the particles are assigned random positions, uniformly distributed on the square, and directions, uniformly distributed on $[-\pi, \pi]$.

For $\eta = 0$ (no noise), if all particles have the same orientation at any instant t_0, they remain perfectly aligned for all $t > t_0$, while for $\eta \geq 1$ the particles cannot form groups and we have a system similar to N independent random walkers. Vicsek and coworkers define the instantaneous order parameter to be the modulus of the average velocity,

$$\varphi(t) \equiv | \frac{1}{N}\sum_{j=1}^{N} e^{i\theta_j(t)} | . \tag{2.3}$$

If the temporal mean of instantaneous order parameter $< \varphi(t) >_t \approx 1/\sqrt{N}$ then the system is composed for N random walkers, while for $< \varphi(t) >_t \approx 1$ then we have an ordered phase with particles moving coherently.

2.2.2 Basic properties

Vicsek and coworkers concluded that the model exhibits a phase transition from the ordered phase to the disordered phase as the noise η is increased. This transition can be easily observed if we measure the time average of the instantaneous order parameter $< \varphi >_t$, varying η. We see in fig.3 that $< \varphi >_t = 1$ if $\eta = 0$ and decays to a small value as we increase the noise. The Fig.3 shows simulation results using $N = 40$ and $L = 3.10$ (blue circles),$N = 100$ and $L = 5.0$ (orange circles) and $N = 400$, $L = 10.0$ (green circles), using 10000 time steps for each value of η.

This model is used to simulate the formation of patterns observed in nature [11]. In fig.4 we see the presence of patterns reproduced by Vicsek model. (a) at t=0 the particles are in random positions, uniformly distributed over the system, and velocities. (b) the

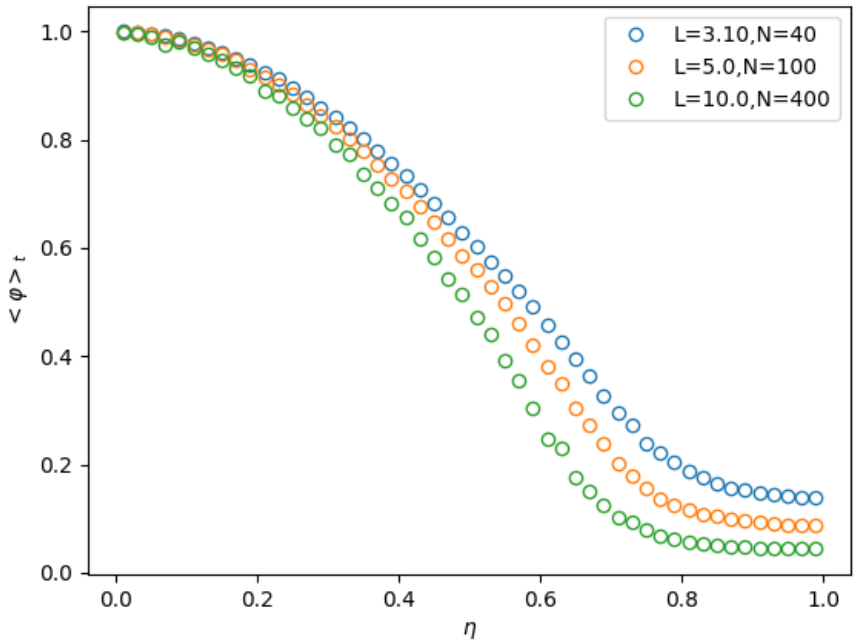

Figure 3 – Temporal average of the order parameter as a function of noise intensity for various values of L.

particles begin to organize themselves and we see the formation of groups. For (a) and (b) L=25 and $\eta = 0.15$; in (c) we observe a coherent motion with the particles moving to the same direction. For (c) L=25 and $\eta = 0.01$.

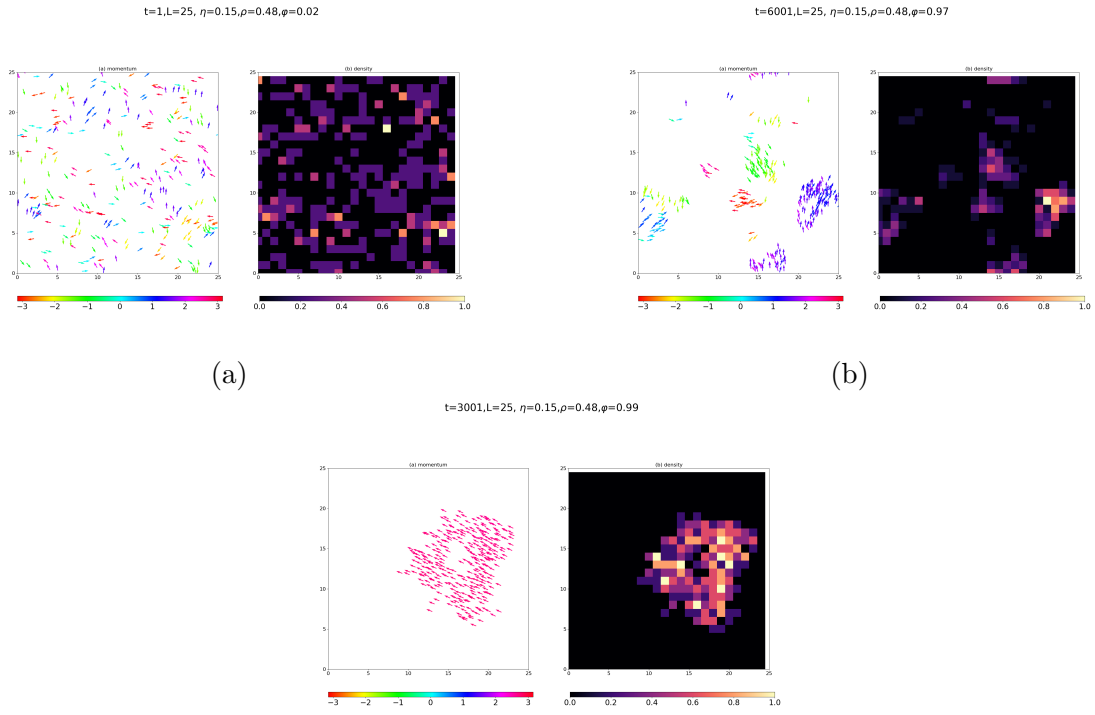

Figure 4 – Typical snapshots of Vicsek model configurations. In all images N=300. (a) t=0; particles have random positions and velocities. (b) For small density and a low noise intensity we observe formation of groups. Here we set $\eta = 0.15$ and L=25. In (c) we see a coherent movement with almost all the particles heading in the same direction. Here we set L=25 and $\eta = 0.01$. The bar below the left image shows the color scale for each angle $\in [-\pi, \pi]$ while the bar below the right image shows the color scale for density in each region.

Vicsek and coworkers stated that the phase transition to collective motion is continuous and similar to the transition to order in an equilibrium spin system, in which η and ρ play the role of temperature and density of spins, respectively. The authors carried out a finite size scaling analysis in order to estimate the critical exponents, i.e, $< \varphi(t) >_t \sim [\eta_c(\rho) - \eta]^\beta$ and $< \varphi(t) >_t \sim [\rho - \rho_c(\eta)]^\delta$. Vicsek and coworkers found the value of $\beta = 0.45 \pm 0.07$ and $\delta = 0.35 \pm 0.06$ for the critical exponents and $\eta_c = 2.9 \pm 0.05$ (In [17] Vicsek et al. use $\eta \in [0, 2\pi]$, with $\rho = 0.4$, for the critical noise.)

2.3 Modifications and subsequent analysis

Due to the success of the VM in reproducing organized motion without a leader, various scientists have studied similar models. Grégoire and Chaté [5] proposed a model based on the VM but with a different implementation of the noise. In the VM, the update of a particle's direction is given by equation 2.2. In this case, the particle makes an error trying to take the mean direction of its neighbors. However, we might imagine that a

significant error arises in determining the direction of motion, θ_k, of each neighbor. This motivated Chaté and Grégoire [5] to propose an updating procedure in which noise is introduced in each such evaluation. In their procedure, referred as *vectorial noise* (VN), the orientation of particle j is updated so:

$$\theta_j(t+1) = \arg[\sum_{k\sim j} e^{i\theta_k(t)} + \eta n_j(t) e^{i\xi_j(t)}], \tag{2.4}$$

where η is the noise intensity, $n_j(t) \geq 1$ is the number of neighbors of particle j at time t and $\xi_j(t)$ is a uniformly distributed random variable in the range $[-\pi, \pi]$.

The factor $n_j(t)$ in equation (2.4) represents the sum of independent contributions associated with each neighbor of particle j. However, in light of central limit theorem, it would be more appropriate to use the factor $\sqrt{n_j(t)}$ instead of $n_j(t)$ since, a sum of n independent contributions has a variance growing $\propto n$ whereas, in equation 2.4, the noise variance grows $\propto n^2$ (See appendix A). Nevertheless, throughout this work I will continue to use the procedure defined by Chaté and Grégoire.

A useful quantity for studying the phase transition is the Binder cumulant,

$$G(\eta) = 1 - \frac{<\varphi^4>}{3<\varphi^2>^2}. \tag{2.5}$$

A convenient property of the Binder cumulant is that it takes known values in the ordered and disordered phases. In addition, it takes negative values if two phases coexist. For a two-component vectorial order parameter ($\vec{\varphi} = \varphi_x\hat{\mathrm{i}} + \varphi_y\hat{\mathrm{j}}$), in the ordered phase $G(\eta) \approx 2/3$ while in the disordered phase $G(\eta) \approx 1/3$. (See appendix B.)

Grégoire and Chaté found that the order parameter (2.3) drops abruptly for vectorial noise and drops smoothly for angular noise. The same happens for the Binder cumulant. We see in Fig.5 the behavior of the order parameter and Binder cumulant, for the two types of noise.

However, the most significant result found by Chaté and Grégoire is that, in fact, the transition is *always* discontinuous, regardless of the type of noise. The qualitative difference observed upon changing the way noise is implemented is only a finite-size effect. The phase transition in the angular noise case reveals its discontinuous character for large system sizes. Fig.6a shows the Binder cumulant as a function of noise intensity (2.2).

We see in Fig.6a that the Binder cumulant attains negative values only for systems larger than L=256, which explains the fact that Vicsek and coworkers [17] understood the phase transition to be continuous: the maximum size simulated by Vicsek et al. in [17] was $L = 128$. Fig.6b shows that, around the critical noise η_c, the distribution function of $\varphi(t)$ is bimodal, confirming phase coexistence, as expected at a discontinuous transition.

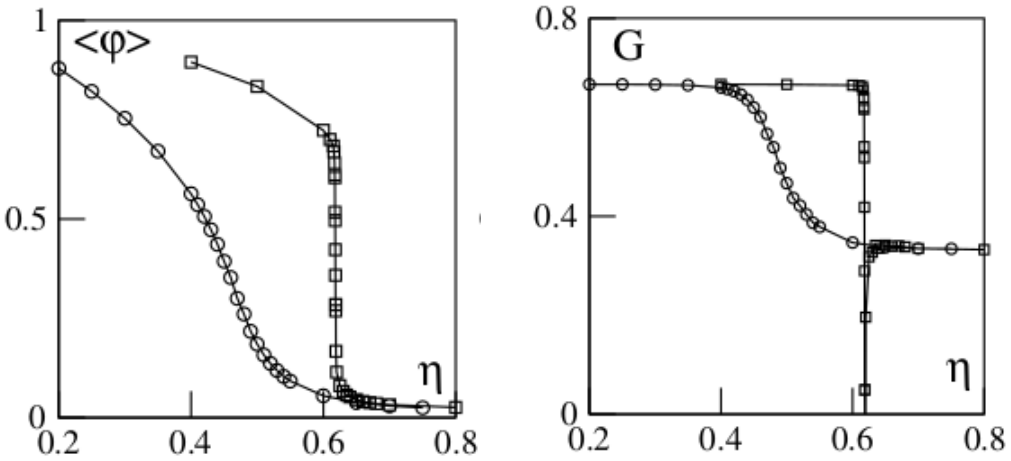

(a) (b)

Figure 5 – Temporal mean of instantaneous order parameter and Binder cumulant for the original Vicsek model (2.2) (circles) and for the vectorial noise model (2.4) (squares) as a function of noise intensity η.($v_0 = 0.5$,$\rho = 2.0$ and L=32.) Figures taken from the article by Grégoire and Chaté [5].

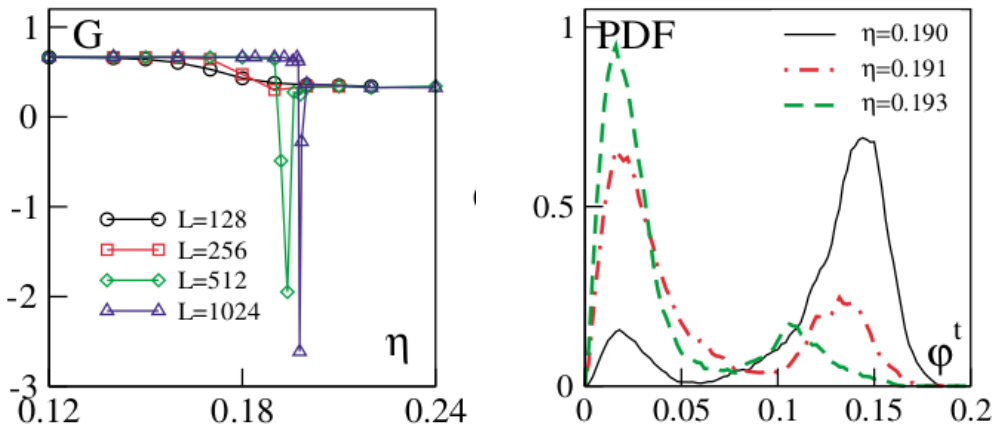

(a) (b)

Figure 6 – Transition discontinuous character for the original Vicsek model with $\rho = 1/8$. (a) G vs η for various sizes of the system and (b) Probability distribution function for some values of η. Figures from Grégoire and Chaté [5].

In a further study Chaté, Ginelli, Grégoire and Raynaud [1] observed high-density bands traveling through a sea of disordered particles, as shown in Fig.7. Bands can be understood as a separation of the ordered phase and the disordered phase. The bands make the phase transition in the VM similar to liquid-vapor coexistence. Near η_c, the time evolution of $\varphi(t)$ is typically as shown in Fig.8, with jumps from the disordered phase to the ordered phase and vice versa. This is further evidence of phase coexistence. The phase diagram for the VM, sketched qualitatively in Fig.9, is composed of three regimes: A disordered one, a (micro)-phase separated ordered regime, characterized by high-density

ordered bands, and the ordered phase.

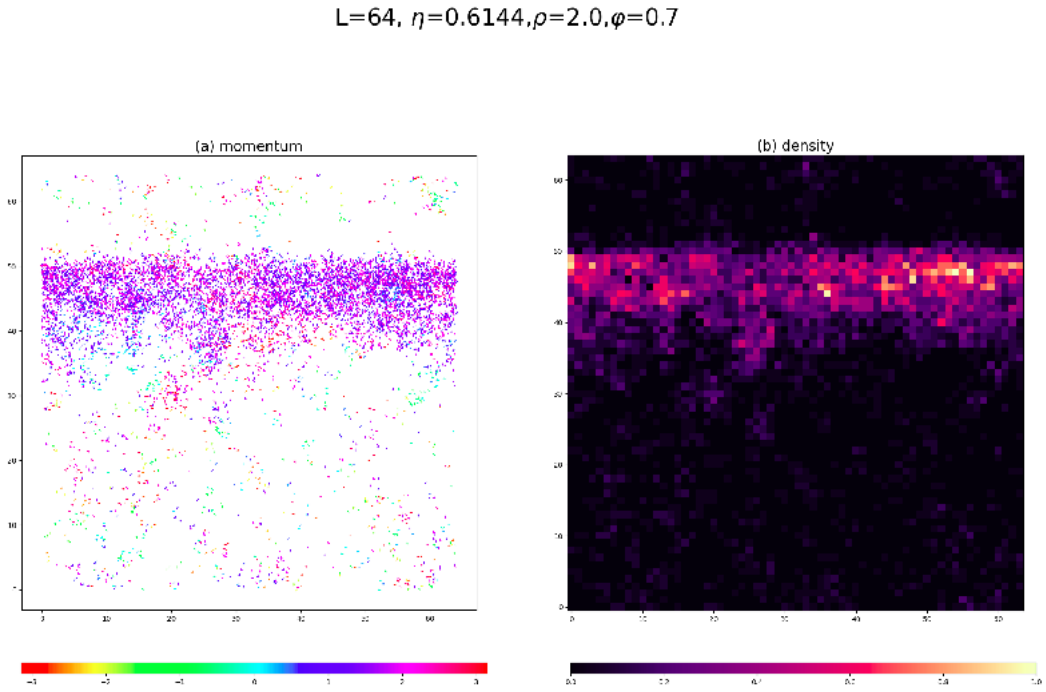

Figure 7 – Typical snapshot of a band in the original Vicsek model with angular noise and parameters: L=64, $\eta = 0.6144$, $\rho = 2.0$ and $v_0 = 0.5$.

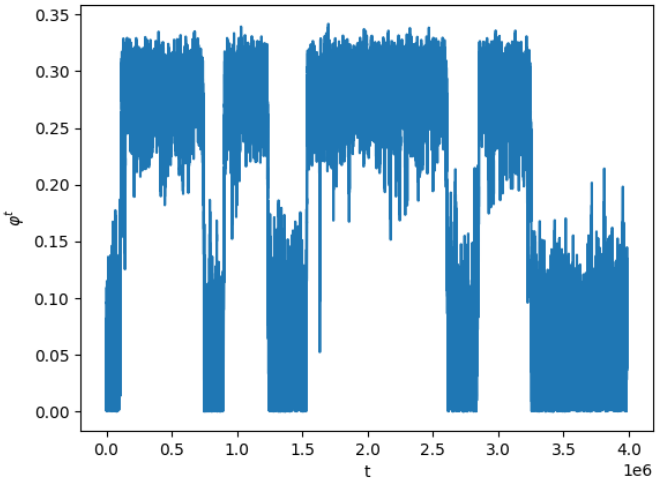

Figure 8 – Order parameter temporal evolution for: $L = 256$, $v_0 = 0.5$, $\rho = 2.0$ and $\eta = 0.475$.

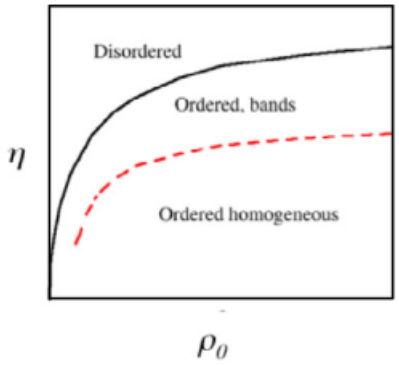

Figure 9 – Qualitative Vicsek model phase diagram. Figure taken from [4].

2.4 Conclusions

The Vicsek model proved to be simple and effective in explaining how individuals moving in groups without communication between them could form patterns and move coherently. Furthermore, Vicsek and coworkers [17] showed that upon increasing the noise intensity there is a transition from the ordered phase to the disordered phase.

In a subsequent analysis, Gregoire and Chaté, after introducing a new implementation of the noise, showed that the transition is discontinuous and only appears to be continuous because of finite size effects. Increasing the size of the system, we observe jumps in the instantaneous order parameter and, between the ordered and disordered phase, there is a phase separation, which is characterized by dense and ordered bands traveling in a sea of disordered particles.

3 Vicsek model with Malthusian population dynamics

3.1 Introduction

Models of population variation have been the subject of study by many scientists from all fields. One of the most important and influential studies in this regard was done by Malthus, in which he concluded that population grew at a faster rate than food production [8]. There are several real systems in which the number of individuals is not conserved, for example, colonies of bacteria [9], intracellular structures, such as the cytoskeleton [7], among other systems.

From the point of view of the hydrodynamic theory of the VM, Toner [13] concludes that it is not possible to find the scaling exponents of the original VM for $d = 2$, but this difficulty can be avoided if we add population dynamics to the VM [12]. Therefore, in this work, we created a computational model in which the interactions between neighbors and the spatial dynamics of each particle would be given by the same equations as the VM, but we added a Malthusian population dynamics. In this chapter I summarize Toner and Tu's hydrodynamic analysis and introduce the VM with Malthusian dynamics.

3.2 Hydrodynamic theory of active fluids

3.2.1 Hydrodynamic analysis of Vicsek Model

Following the article by Vicsek and coworkers [17], Toner and Tu (T&T) [14] [16] published a hydrodynamic analysis inspired by the model. The authors seek to understand if in a model of self-propelled particles is possible to have a stable ordered phase, considering that such phase is ruled out in a 2D equlibrium system by the Mermin-Wagner theorem [10]. Toner published a reanalysis of the problem, in which the authors added terms that they missed in [14]- [16]. In this new analysis [13], the author starts with the set of equations below:

$$\partial_t \vec{v} + \lambda_1(\vec{v}\cdot\nabla)\vec{v} + \lambda_2(\nabla\cdot\vec{v})\vec{v} + \lambda_3\nabla(|\vec{v}|^2) = \alpha\vec{v} - \beta|v|^2\vec{v} - \nabla P_1 - \vec{v}(\vec{v}\cdot\nabla P_2) + D_1\nabla(\nabla\cdot\vec{v}) + D_T\nabla^2\vec{v} + D_2(\vec{v}\cdot\nabla)^2\vec{v} + \vec{f}, \tag{3.1}$$

$$\partial_t\rho + \nabla\cdot(\vec{v}\rho) = 0, \tag{3.2}$$

where $\overrightarrow{v}$ and ρ are the velocity and density field, respectively, β, D_1, D_2, D_T are positive constants and $\alpha < 0$ and $\alpha > 0$ represent the disordered and ordered phases, respectively. In the ordered phase: $< |v| >= \sqrt{\alpha/\beta} \neq 0$. $D_{T,1,2}$ are diffusion constants and the Gaussian noise $\overrightarrow{f}$ has properties:

$$< f_i(\vec{r}, t) >= 0,$$
$$< f_i(\overrightarrow{r}, t) f_j(\overrightarrow{r'}, t') >= \Delta \delta_{ij} \delta^d(r - \vec{r'}) \delta(t - t'),$$

where Δ is the noise amplitude. Eq.(3.2) is the continuity equation, while (3.1) generalizes the Navier-Stokes equation, including, in the terms $\propto \alpha$ and β, a phenomonological description of Landau-type ordering. And finally, we expand the isotropic pressure P_1 and the anisotropic pressure P_2 around the equilibrium density ρ_0:

$$P_1 = P_1(\rho, |\overrightarrow{v}|) = \sum_{n=1}^{\infty} \sigma_n(|\overrightarrow{v}|)(\rho - \rho_0)^n,$$
$$P_2 = P_2(\rho, |\overrightarrow{v}|) = \sum_{n=1}^{\infty} \mu_n(|\overrightarrow{v}|)(\rho - \rho_0)^n.$$

It is interesting to note that T&T missed some terms in [14]- [16], such as the pressure P_2 that has to be included because the system is out of equilibrium. As we are interested in the ordered phase, we can write the velocity field as,

$$\overrightarrow{v} = v_0 \hat{x}_{||} + \delta \overrightarrow{v} = (v_0 + \delta v_{||}) \hat{x}_{||} + \overrightarrow{v}_{\perp},$$

where $v_0 \hat{x}_{||} =< \overrightarrow{v} >$ is the mean velocity in the ordered phase; $\delta v_{||}$ and $\overrightarrow{v}_{\perp}$ are the fluctuations of the velocity parallel and perpendicular to the mean velocity, respectively.

In this text, we just discuss the main results of [13]. Reproducing all the development of the authors would be lengthy. To begin, Toner only maintain terms of linear order of $\overrightarrow{v}_{\perp}$ and $\delta\rho$. In this regime, they simply find the same results as [14]- [16], in which, the main result is that, in the linearized analysis, the Mermin-Wagner theorem [10] prohibits an ordered phase in two dimensions. So far the new terms, which were missed in [14]- [16], and which were added to the 3.1 equation, do not change anything compared to the previous analysis, if we approximate the fluctuations by linear terms.

In [14]- [16] the authors noticed that nonlinearities and fluctuations completely change the scaling behavior at long wavelength. While this prediction is correct, others are invalidated by the other nonlinearities overlooked in [14]- [16]. In order to analyze the effect of the nonlinearities on the long length and time scales for d<4 , T&T rescale

length, time and fields $\hat{v}_\perp$ and $\delta\rho$ to:

$$\begin{aligned} \hat{x}_\perp &\to b\hat{x}_\perp \\ x_{||} &\to b^\zeta x_{||} \\ t &\to b^z t \\ \hat{v}_\perp &\to b^\chi \hat{v}_\perp \\ \delta\rho &\to b^{\chi_\rho}\delta\rho. \end{aligned} \tag{3.3}$$

In this analysis, the stable ordered phase is only possible if $\chi < 0$. In [14]- [16], T&T had determined this exponents in a fixed point and found that the nonlinearities imply $\chi = -1/5$. In [13], including the terms overlooked in previous articles, for $d > 4$ all of the nonlinearities flow to zero, hence the linearized theory is correct at long length and time scales. However, for $d < 4$, Toner found that the nonlinearities grow, invalidate the linearized analysis and make impossible to determine the scaling exponents.

3.2.2 Vicsek Model with population dynamics

In addition to the experimental and simulational importance of systems that do not conserve the number of individuals [7] [9], this type of system has some additional features that make it especially important. As shown by Toner and Tu [13] and discussed briefly in section 3.2.1, the VM with immortal individuals has nonlinearities that make it impossible to evaluate the scaling exponents. These difficulties can be avoided if we allow the number of individuals to vary.

The starting point is equation 3.1 where, again, the pressures and other parameters are functions of ρ and $|v|$. We expand the pressures $P_{1,2}$ about ρ_0 as: $P_i(\rho) = P_i^0 + \sum_{n=1}^{\infty}\sigma_{i,n}(|\overrightarrow{v}|)\delta\rho^n$ where $i = 1, 2$. The noise is the same as in 3.2.1 and the absolute velocity in the ordered phase is the same, $v_0 = \sqrt{\alpha/\beta}$.

We now need an equation of motion for ρ. In immortal flocks, this is just the usual continuity equation 3.2 of compressible fluid dynamics. For Malthusian flocks, it needs include the effect of birth and death. Let's also assume that the death rate increases with density. Let $g(\rho)$ be the density growth rate in the absence of motion; g vanishes for $\rho = \rho_0$,and $g(\rho) < 0$ $\rho > \rho_0$; $g(\rho) > 0$ for $\rho < \rho_0$. So, the equation of motion for density is:

$$\partial_t\rho + \nabla\cdot(\overrightarrow{v}\rho) = g(\rho).$$

Using a dynamical renormalization group (RG) analysis [12], Toner concludes that it is possible to obtain all the scaling exponents for $d = 2$ via the following relations:

$$z - 2\zeta = 0, \quad z - \zeta - 2\chi + 1 - d = z - \zeta - 2\chi - 1 = 0.$$

These relations and $\chi = 1 - z$ (which comes from requiring that graphical corrections vanish in RG) implies,

$$z = \frac{6}{5}, \quad \zeta = \frac{3}{5}, \quad \chi = -\frac{1}{5}.$$

The main interest in knowing the exact values of the scaling exponents is to understand how the correlation functions decay and, in principle, it is possible to determine these exponents in simulations. Thus, the theoretical advantage of studying the system with population dynamics is made clear by the fact that we can calculate its scaling exponents, differently from the original VM. In the next section, we introduce a theoretical model that has the same premises as Toner's model [12], in order to study a Vicsek like model with population dynamics in computer simulations.

3.3 Construction of the Model

We need to create a model that is plausible to be implemented computationally and takes into account all possible aspects of the Malthusian Toner model. The equations for the temporal evolution of positions and directions are the same as those of the original VM introduced in the section 2.2; For covenience I recall them here.

The model has the same definitions than the VM, including the constant speed v_0, the boundary conditions and the temporal evolution in discrete steps Δt. The position of particle j is updated so:

$$\mathbf{x}_j(t + \Delta t) = \mathbf{x}_j(t) + \mathbf{v}_j \Delta t, \tag{3.4}$$

where $\mathbf{v}_j = (v_0 \cos\theta_j, v_0 \sin\theta_j)$. The direction θ_j is updated as the average of the angles of the particles in its neighborhood (including itself). The neighborhood of the j-th particle is defined as every individual with a distance less than or equal R_0 of the particle in question. The equation for updating the direction with angular noise (AN) and vectorial noise (VN) are below:

$$\theta_j(t + \Delta t) = \arg[\sum_{k\sim j} e^{i\theta_k(t)}] + \eta\xi_j(t), \qquad (AN) \tag{3.5}$$

$$\theta_j(t + \Delta t) = \arg[\sum_{k\sim j} e^{i\theta_k(t)} + \eta n_j(t) e^{i\xi_j(t)}], \quad (VN) \tag{3.6}$$

where the sum is over all particles in the neighborhood of the particle j; η is the noise intensity, $n_j(t)$ is the number of neighbors of j at time t and $\xi_j(t)$ is a uniformly distributed random variable on the interval $[-\pi, \pi]$.

Without loss of generality we can fix $R_0 = \Delta t = 1$. So far the model is completely the same as the VM. Now we define the population dynamics. At each time step, we choose n_e particles that will participate of the population dynamics. n_e is a random number drawn from a Poisson distribution with mean $m_e = N(t)/\nu$, where N(t) is the number of

particles in time t, and ν is a parameter. Note that the larger ν, the fewer particles will participate in the population dynamics. (For example, if we set $\nu = 2$, on average, half of the particles will participate.) When a particle is chosen it either dies or reproduces. Particle j dies with probability p_j^d given by :

$$p_j^d = \frac{n_j(t)\gamma}{1 + n_j(t)\gamma}, \tag{3.7}$$

where $n_j(t)$ is the number of neighbors within a radius R_d at time t and γ is a parameter. With complementary probability $1 - p_j^d$, the particle reproduces. We fix $R_d = 1$ in this study.

The particle is created in a random position close to its parent; it's position is given by,

$$\vec{\mathrm{x}}_j = \vec{\mathrm{x}}_{parent} + \overrightarrow{\sigma}, \tag{3.8}$$

where $\vec{\mathrm{x}}_{parent}$ is the position of the parent, $\overrightarrow{\sigma}$ is uniformly distributed over the disk of radius r_d. In this work we set $r_d = 0.5$, while the direction of the born particle is chosen randomly in the range $[-\pi, \pi]$. Thus, our model, unlike the VM, has four parameters: v_0, η, ν and γ.

4 Computational Methods

4.1 Introduction

Computational methods are used in different areas of science to understand and solve problems that are too complex to solve analytically. There are several algorithms that allow simulating physical systems, but here we focus on Monte Carlo simulations. A Monte Carlo simulation is the name given to any computer simulation that uses random numbers to simulate a process in order to estimate something about the outcome of that process. We do not intend discuss in details Monte Carlo simulations in here, in case the reader is interested in a further discussion,please consult appendix C.

The principal difficulty in simulating the Vicsek model is cost. In naive a algorithm the simulation time grows $\propto N^2$, where N is the number of particles. As we use N of order 10^5, this would be unfeasible. To avoid this problem, we use an algorithm in which the system is divided into cells, that the simulation time scales with $O(N)$. In this section we present the main computational aspects of the VM with population dynamics. We discuss the algorithm, the random number generator, the programming language and other aspects.

4.2 Simulation of the Vicsek Model with population dynamics

The Vicsek model is simple and quite suitable for computational studies: equations 3.4, 3.5 and 3.6 can be easily implemented in a computer. However, the condition for particle j to be neighbor to particle i is: $d^2 < R_0^2$, where $d^2 = (x_i - x_j)^2 + (y_i - y_j)^2$ where x and y are the position of each particle in Cartesian coordinates. Therefore, if we test all pairs of particles to check if they are neighbors, this implies the simulation time $\propto N^2$. We can write the algorithm for this part of the program as follows:

Algorithm 1 Calculation of neighbors by brute force

```
n(i)=0                                          ▷ Number of neighbors of i
for  i= 1 to N do
    for  j= 1 to N do
        d^2 = (x(i) − x(j))^2 + (y(i) − y(j))^2
        if d^2 < R_0^2 then
            n(i) = n(i) + 1
```

Two loops over N particles make a brute force neighbor calculation cumbersome; hence we adopt another algorithm for neighbor calculation. First, the system of area L^2 is divided into L^2 boxes of size $R_0 = 1$, called cells.

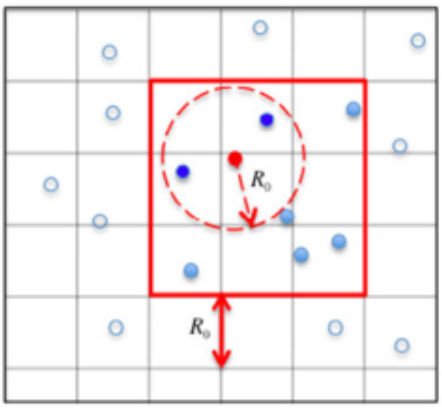

Figure 10 – Division of the system into cells. Dark blue circles are particles that are in neighboring cells and within the neighboring radius; Light blue circles that are in neighboring cells but not in the neighborhood radius; Transparent particles that are not in neighboring cells. Image taken from the reference [4].

Fig.10 shows a scheme representing this division into cells and, with the system divided, each particle is assigned a cell each time step. Once this is done, it is clear that for any given particle i, all other particles lying outside the box containing i and its next neighbouring boxes cannot be closer than R_0. Making these improvements, the computational time grows $\propto N$. This algorithm allows us to calculate the mean in the equations 3.5 and 3.6 and determine the new direction of each particle.

In addition to the algorithm for neighboring particles described above, we created an algorithm for population dynamics. First, we draw n_e random particles, from a Poisson distribution with mean $m_e = N(t)/\nu$, which are the particles that participate in the population dynamics at time t. For this we use a code that creates random samples of various probability density functions, known as RANLIB. We select the RANLIB function IGNPOI and specify the mean of the Poisson distribution. The code returns a number from this distribution.

We then select n_e particles and, having the number of neighbors of each one of them. We calculate p_j^d given by 3.7 for a particle, and we draw a pseudorandom real

number p_e in the range $[0, 1]$. After that, we have a condition: If $p_e < p_j^d$ the particle dies, otherwise a particle is born under the conditions given in section 3.3. Another rule of the program is that when a particle is born at time t it cannot be selected for population dynamics nor count as a neighbor of other particles until the next time step.

For both population dynamics and adding noise to update the direction of motion, we need pseudorandom numbers. For this we use the pseudorandom number generator *random_number* which generates a real number in the range $[0, 1]$. The period of this generator is $2^{256} - 1$ which is sufficient for simulations with at most 5×10^6 time steps and the number of particles on the order of 10^5.

The entire program is written in FORTRAN90 and the compiler used was *gfortran*. The programs were run on the computational system of Statistical Physics-UFMG cluster. The complete code can be found in E.

5 Results

5.1 Introduction

In this chapter we present the results obtained from computational simulations of the model described in section 3.3. To begin, we analyze how the formation of groups affects the measured quantities and how the system depends on the parameters γ and ν, which control population dynamics. Afterwards, we look at the transition between the ordered and disordered phases, trying to understand how this transition occurs. Finally, we discuss the role of bands and how they are affected by population dynamics. We study the model with the two types of noise, angular noise (AN) 3.5 and vectorial noise (VN) 3.6, and in the regime of low and high speeds.

5.2 Relation between the stationary density ρ_s and the parameter γ, which controls the death probability

First of all, let's examine what happens to ρ_s when we vary γ, introduced in Eq.(3.7), maintaining the noise intensity η constant. As we can see in Fig.11, particles tend to form clusters, leaving most of the space empty, as γ is increased.

In Fig. 12 it is clear that for $\eta \geq 0.3$, ρ_s is inversely proportional to γ, while for $\eta \leq 0.3$, $\rho_s \propto \frac{1}{\gamma^\lambda}$ with $\lambda > 1$. The reason is that for $\eta \geq 0.3$ the density is almost uniform, regardless of γ, whereas for $\eta < 0.3$ the particle distribution is nonuniform for small values of γ: Fig. 12 shows that ρ_s is an increasing function of η, because increasing noise suppresses clustering. In the steady state, the mean death probability is: $p^d = 1/2$ and, by Eq.(3.7), the number of neighbors of j is $n = 1/\gamma$. When the particles are uniformly distributed, on average, the particles have the same number of neighbors, so that,

$$\rho_s = 1/\gamma\pi. \tag{5.1}$$

From Fig.12 we see that this relation is true for $\eta \geq 0.5$ with angular noise and $\eta \geq 0.7$ for vectorial noise, because for these values of η, the particles are uniformly distributed.

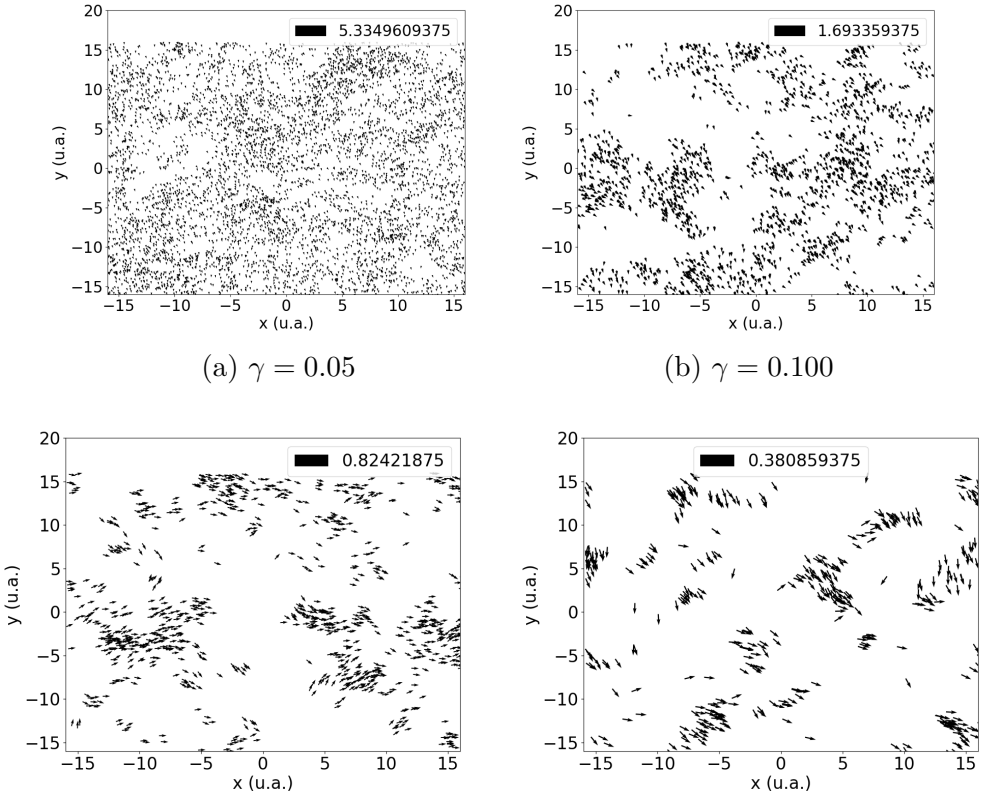

(a) $\gamma = 0.05$ (b) $\gamma = 0.100$

(c) $\gamma = 0.150$ (d) $\gamma = 0.200$

Figure 11 – Typical configurations for: $\eta = 0.1$, $\nu = 100$, $L = 32$ and γ as indicated.

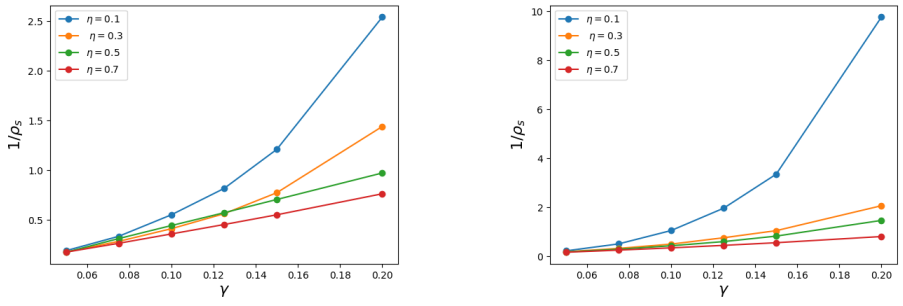

(a) (b)

Figure 12 – Reciprocal of stationary density versus γ for: $L = 32$, $\nu = 100$ $v_0 = 0.5$ and η as indicated, For (a) AN and (b) VN. Time averages were computed over $2\text{x}10^5$ time steps.

5.3 Relation between population dynamics and noise

Particle creation or removal disturbs orientational order, since each newly created particle is assigned a random direction of motion, uniform on $[-\pi, \pi]$. This motivates a study of the temporal evolution of the mean orientation $< \theta >$. Fig. 13 shows that

the mean angle fluctuations are greater, the smaller ν, i.e., more rapidly the population dynamics proceeds. Fig. 13 (a) shows data for $\gamma = 0.150$ while in (b) $\gamma = 0.100$. We see that the fluctuations are stronger in (a) than in (b). This is expected since for a smaller number of particles, noise due to population dynamics has a stronger effect.

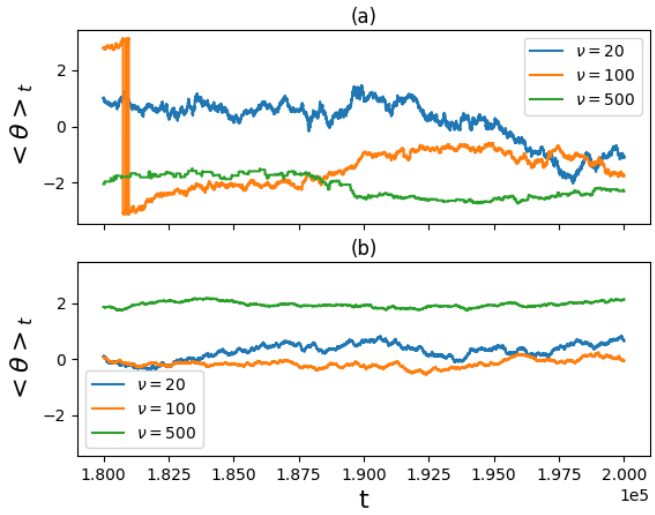

Figure 13 – Evolution of the mean angle for three different system with $\eta = 0.0$,$v_0 = 0.5$, $L = 20$ and ν as indicated. Panel (a) $\gamma = 0.150$; (b) $\gamma = 0.100$

5.4 Orientational persistence and population dynamics

Next, we look at how long particles maintain their orientation. Let $< \theta > (t)$ be the mean angle (over all particles) at time t, and let

$$\Phi(\tau) \equiv \left\langle e^{i[<\theta>(t+\tau)-<\theta>(t)]} \right\rangle , \tag{5.2}$$

where the outer average is over. We can understand $\Phi(\tau)$ as a measure of the correlation between the mean angle $< \theta > (t)$ and $< \theta > (t + \tau)$. In systems with few particles and small η (see Fig.14), faster population dynamics leads to a more rapid decay of global orientational correlations.

If we increase η, this effect should be weaker, since the noise caused by population dynamics affects a small fraction of the particles at each time step, while increasing η affects all particles. Fig. 15 shows $\ln \Phi$ as a function of τ for $\eta = 0.3$; we see that the effect of population dynamics is not as noticeable as for $\eta = 0.05$, as expected.

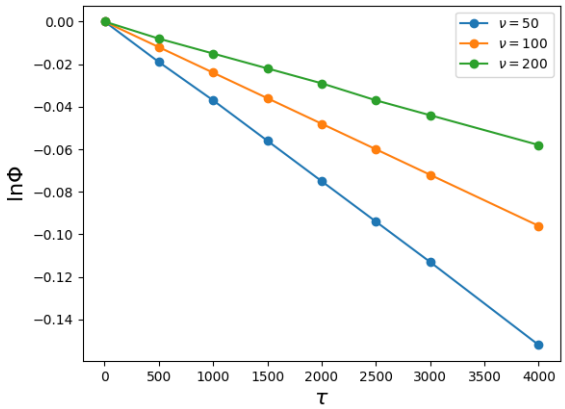

Figure 14 – $\ln \Phi$ versus of τ for: $\eta = 0.05$, $L = 16$, $\gamma = 0.2$ and ν as indicated.

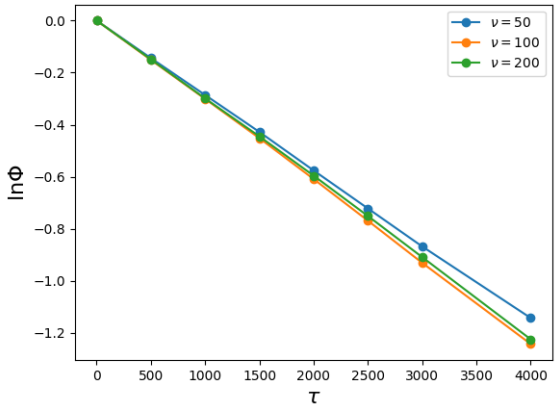

Figure 15 – $\ln \Phi$ versus of τ for: $\eta = 0.3$,$L = 16$,$\gamma = 0.1$ and ν as indicated.

5.5 The phase transition

In this section, we examine the transition from the ordered to the disordered phase in more detail and how population dynamics affects the phase transition. As an overture, we analyze systems with fixed $\gamma = 0.1$, $v_0 = 0.5$, and two values of ν, $\nu = 20$ and $\nu = 100$. All simulations in this section are done with VN (3.6). First of all, we see that the time averaged scalar order parameter $< \varphi >_t$ displays a sharp drop (see Fig.16a-16b), and that the Binder cumulant exibits a minimum at the transition point (Fig.16c-16d), indicating a discontinuous phase transition. In addition, the variance of instantaneous oder parameter is almost delta-peaked as in VM with VN [1](Fig.16e-16f).

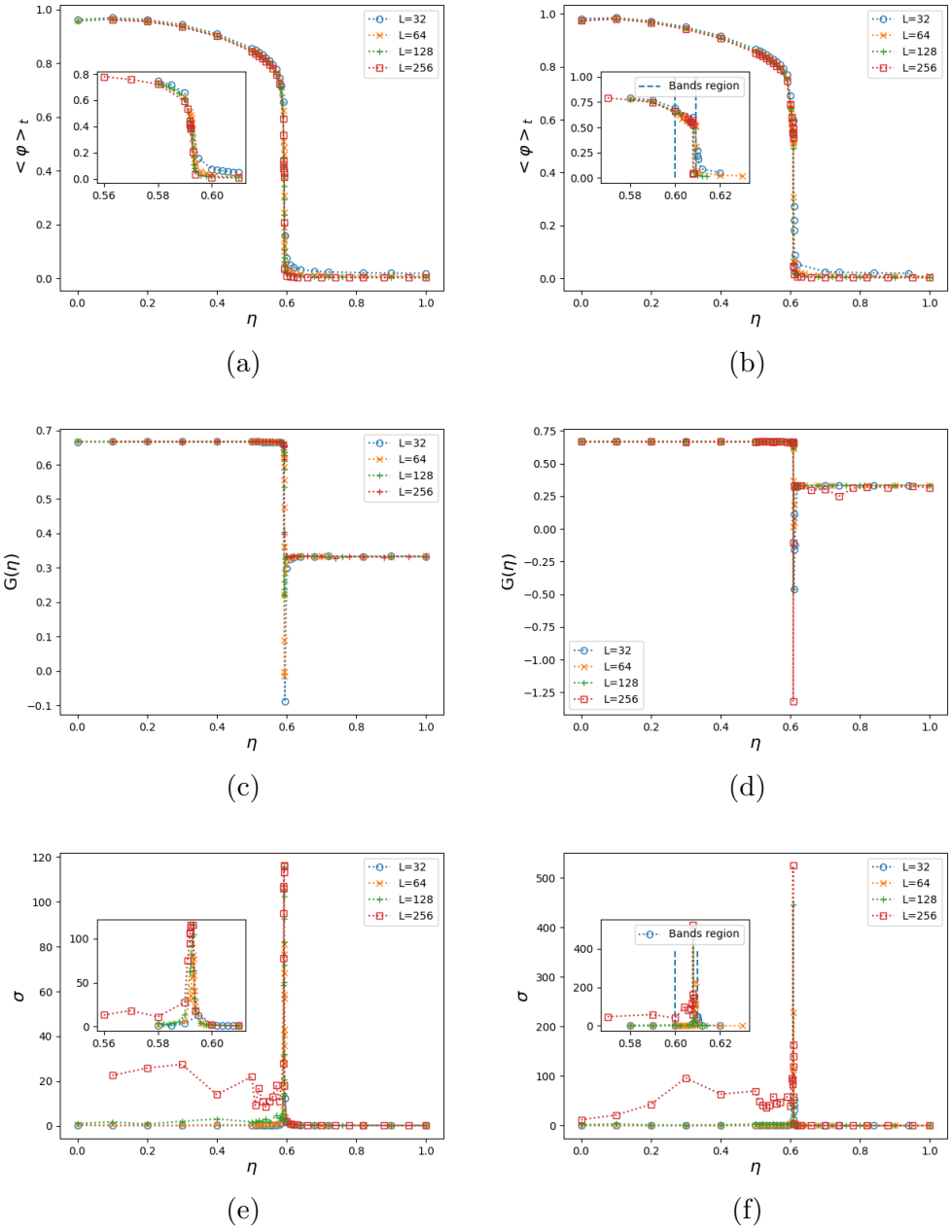

Figure 16 – Order parameter, Binder cumulant and variance versus noise intensity for: $v_0 = 0.5$, $\gamma = 0.1$ and L as indicated. (a) and (b) show the order parameter as a function of η for $\nu = 20$ and $\nu = 100$ respectively, while (c) and (d) show the stationary density versus η to ν as in (a) and (b). (e) and (f) show the variance of instantaneous order parameter for $\nu = 20$ and $\nu = 100$, respectively.

5.5.1 Hysteresis

Hysteresis is a classic phenomenon observed in the vicinity of discontinuous phase transitions. When we increase or decrease the intensity of the noise passing through the transition point, a hysteresis loop is formed. Fig. 17 shows the effect on the order parameter and density for three different values of ν. Hysteresis becomes weaker as we decrease ν.

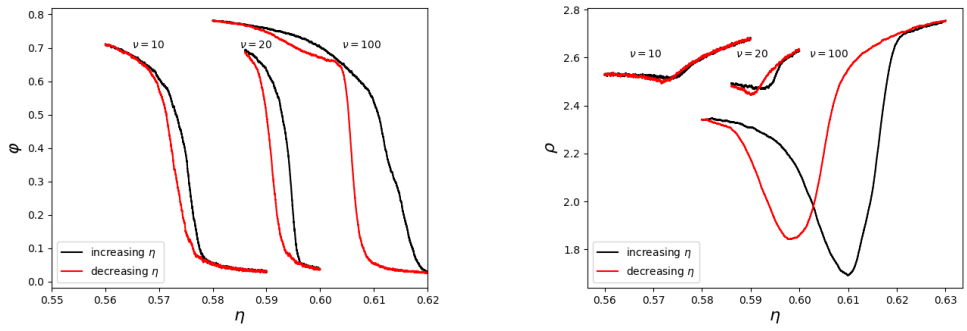

(a) (b)

Figure 17 – The hysteresis loop for three different values of ν for: $L = 64$, $\gamma = 0.1$, $v_0 = 0.5$. (a) shows the effect for the order parameter and (b) for the density. The increase/decrease rate is $2\text{x}10^{-6}$ per time step.

We graphically represent the density as a function of the order parameter, as shown in Fig. 18. We can see a huge difference between the behavior of $\nu = 100$ and $\nu = 20$ or $\nu = 10$, again this is due to bands.

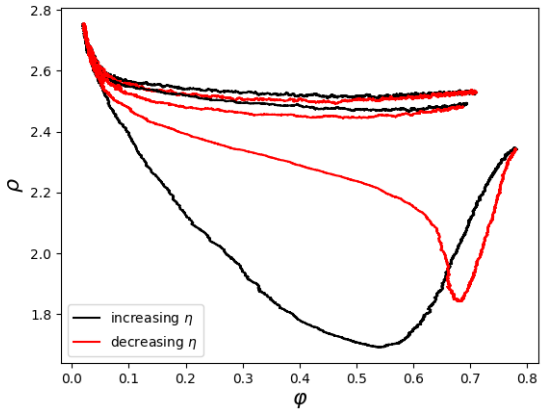

Figure 18 – Density versus order parameter for η changing over time with a constant rate of increase/decay. The two curves below are for $\nu = 100$; in the middle $\nu = 20$; On top $\nu = 10$.

5.5.2 How the rate of population dynamics affects the phase transition

First, we examine the dependence of stationary density on noise intensity for fixed ν and γ. Fig. 19a-19b shows that ρ_s grows with η until η reaches the transition region, where the density starts to decrease, and after this region, as η is increased ρ again increases, saturating when η approaches 1, at a value close to $1/\gamma\pi$. As we have already see the section 5.2, this is the stationary density for uniformly distributed particles. We see in Fig.19a-19b that the transition occurs to a slightly smaller η for $\nu = 20$ compared to

$\nu = 100$. This is due to the fact already discussed in section 5.3; the smaller ν, the larger the effective noise caused by the population dynamics.

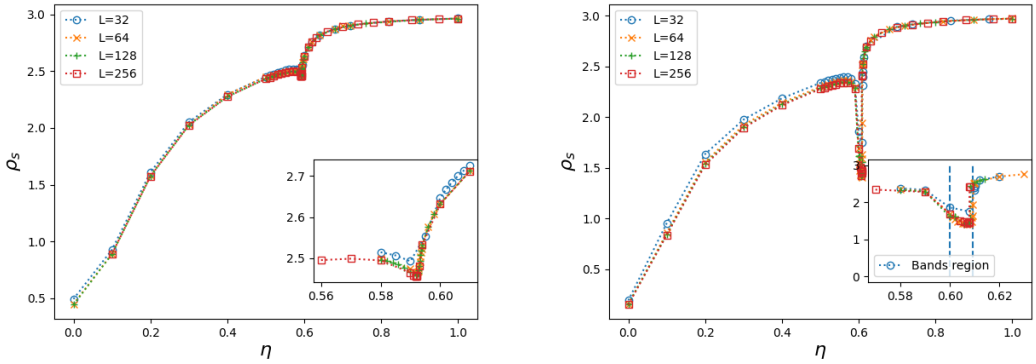

(a) (b)

Figure 19 – Stationary density versus noise intensity for: $v_0 = 0.5$, $\gamma = 0.1$; (a)$\nu = 20$, (b) $\nu = 100$ and L as indicated

Before and after the transition region, this makes sense because the particles become more uniformly distributed as η is increased, so that particles reproduce/die and tend to density near $1/\gamma\pi$. If particles form groups (as happens for small η), there are empty regions.

To understand how noise intensity affects particle distribution, we calculated cell occupancy histograms. We divide the system into L^2 square cells of unit area. Let $P_{cell}(x)$ be the probability that a cell contains exactly x particles. The histogram in Fig. 20 shows that particles tend to cluster, leaving most cells empty for small noise intensities; when $\eta \simeq 1$ then the histogram is unimodal with a peak close to ρ_s, as shown in Fig. 21. With these parameters, the density is $\rho_s \simeq 2.0$ and $\rho_s \simeq 3.2$ for the histograms of Fig(20) and Fig.(21) respectively. In the latter case, a Poisson distribution with intensity ρ_s provides an excellent fit for the data, as expected for the disordered phase.

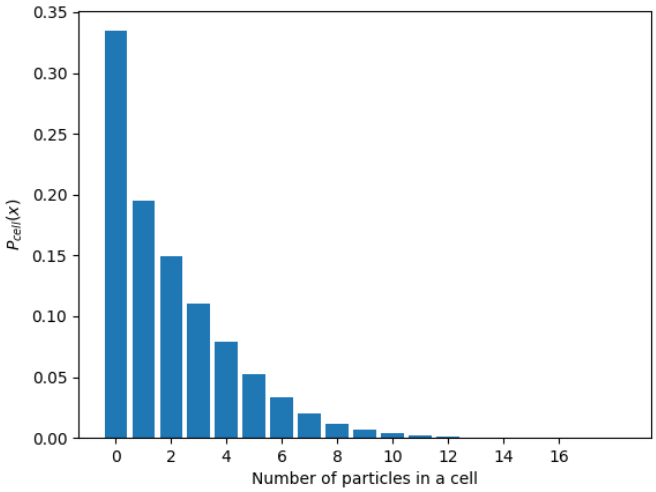

Figure 20 – Cell occupancy histogram for: $\eta = 0.1$, $v_0 = 0.5$, L=16 and $\gamma = 0.1$.

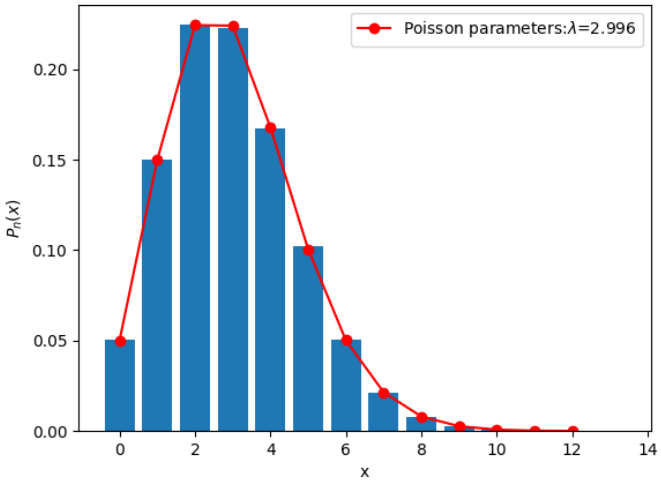

Figure 21 – Cell occupancy histogram for: $\eta = 1.0$, $v_0 = 0.5$, L=16 e $\gamma = 0.1$.

Besides to adding a new noise source to the original VM, population dynamics affects the emergence and persistence of bands. The ordered phase of the VM is characterized by high-density moving bands. Since a fraction $1/\nu$ of the particles participate on average in the population dynamics at each time step, $1/\nu$ effectively represents the general rate of this process. Thus, varying ν can be expected to have a strong effect on order. This is evident in Fig. 22-23: for $\nu = 100$, the bands are present, while for $\nu = 20$ they are absent. Fig.22 shows some configurations for $\nu = 20$ and $\nu = 100$ close to η_c. Again, bands appear for $\nu = 100$ and do not for $\nu = 20$. As population dynamics tends to make the number of neighbors $1/\gamma$ in the neighborhood, of each particle, if population dynamics occurs at a sufficiently high rate, density fluctuations become negligible which suppresses the bands.

However, how quickly the fluctuations are eliminated depends on ν, and therefore, for large values of ν, population dynamics cannot uniformize the density.

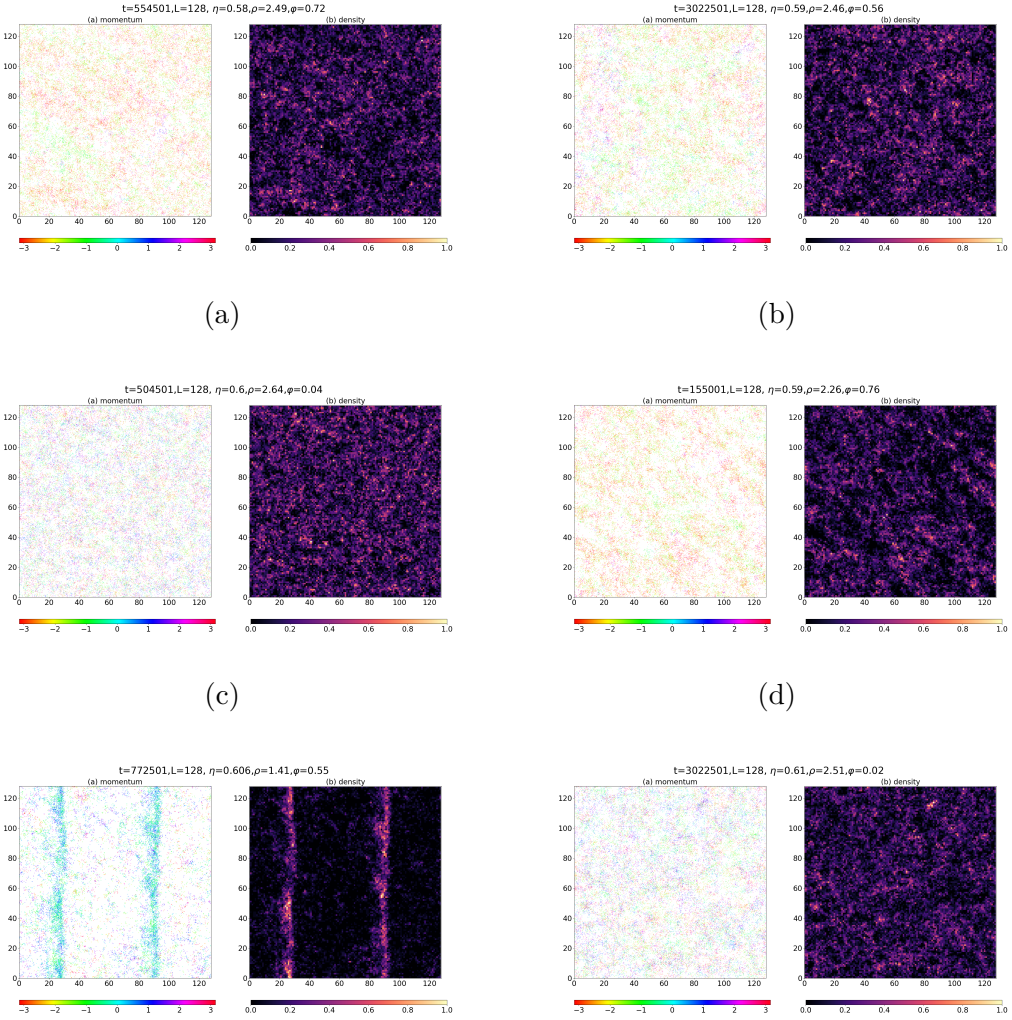

Figure 22 – Typical configurations for: $v_0 = 0.5$, $\gamma = 0.1$. In (a),(b) and (c) $\nu = 20$ and $\eta = 0.58$,$\eta = 0.59$ and $\eta = 0.60$ respectively; For (d), (e), (f) $\nu = 20$ and $\eta = 0.59$, $\eta = 0.606$ and $\eta = 0.62$ respectively. The colors represent the directions of particles in the range $[-\pi, \pi]$.

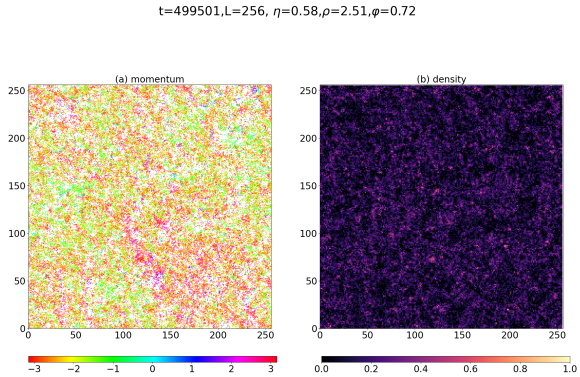

(a)

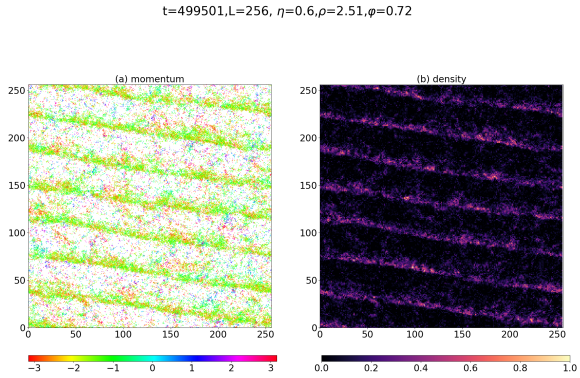

(b)

Figure 23 – Typical configuration of the ordered phase. (a) represents the moments and (b) is the normalized density field. The colors indicate the angle of each particle in the range $[-\pi, \pi]$ (Below the left image) and indicate the normalized denssity field in $[0, 1]$. Both images have: L = 256, $v_0 = 0.5$ and $\gamma = 0.1$. In (a), we define $\nu = 20$ and $\eta = 0.5800$, while (b) $\nu = 100$ and $\eta = 0.6000$.

The small difference in the value of η for the two images is a consequence of trying to capture snapshots at the transition point (η_c), but the transition points are different, as the effective noise is different for each value of ν (see section 5.5).

In order to understand the different behavior in η_c for different values of ν, let's construct a neighbors histogram. Let $P_n(x)$ be the probability of a particle has x neighbors, then we plot $P_n(x)$ as a function of the number of neighbors as shown in Fig.24. We observe in Fig.24(a) that $P_n(x)$ is unimodal centered on $1/\gamma$, as the majority of particles have almost the same number of neighbors, there is no density fluctuation; For $\nu = 100$ we observe density fluctuations associated with the bands. In Fig.24(b) we see that the distribution of neighbors is not unimodal, we have a large amount of particles with a low number of neighbors (in relation to $1/\gamma$=10) and some amount of particles with a high number of neighbors. This is because when we set $\nu = 100$ the rate of population dynamics is slow enough to allow for fluctuations in density. We define the following quantity to

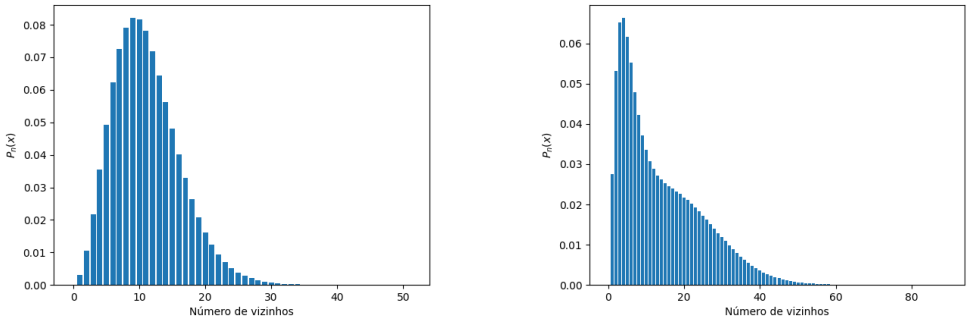

(a) (b)

Figure 24 – Histogram of the number of neighbors for: $\gamma = 0.1$,$L = 128$. In (a) $\nu = 20$ and $\eta = 0.5934$ and in (b)$\nu = 100$ and $\eta = 0.6082$.

measure the non-uniformity of the particle ditribution:

$$\tilde{p} \equiv \frac{\text{var}[n]}{< n >} - 1, \tag{5.3}$$

where n is the number of particles in a cell of unit area. $\tilde{p}$ is zero if n has a Poisson distribution and increases as the non-uniformity is increased. Fig.25 shows that for $\nu = 100$ the distribution is more non-uniform than for $\nu = 20$, and that exhibits a sharp peak at phase transition.

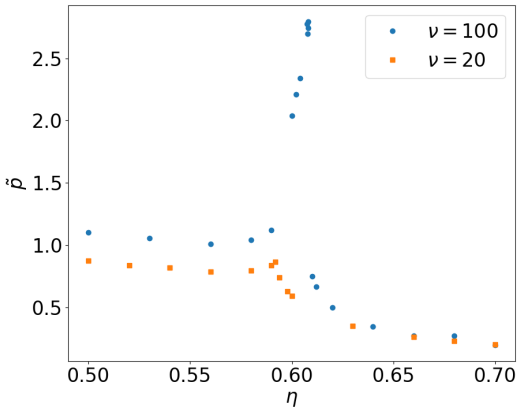

Figure 25 – $\tilde{p}$ versus η for: $L = 128$, $\gamma = 0.1$ and ν as indicated.

Furthermore, bands are the reason for the drop in stationary density when η reaches the transition regime. In each band the density is very high, while outside the density is much lower, consistent with the scenario of coexistence between a dense ordered phase and a rarefied disordered phase, hence the global density decreases. We see in Fig.26 that the probability distribution for the instantaneous order parameter is bimodal for $\nu = 100$ and unimodal for $\nu = 20$. In addition, Fig.28 shows the temporal evolution of the order parameter near the transition point. We see that the order parameter jumps from the

disordered to the ordered phase when $\nu = 100$, whereas jumps are not observed for $\nu = 20$. In Fig. 28 we see that when the system switches to the ordered phase the density decreases.

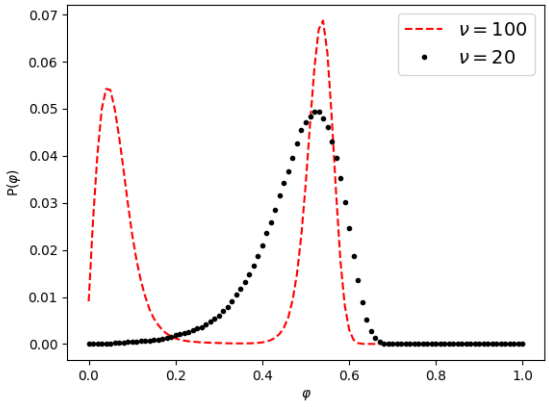

Figure 26 – Probability distribution of the instantaneous order parameter for: $L = 64$, $\gamma = 0.1$ and ν as indicated. For $\nu = 20$ and $\nu = 100$, $\eta = 0.5934$ and $\eta = 0.6094$, respectively.

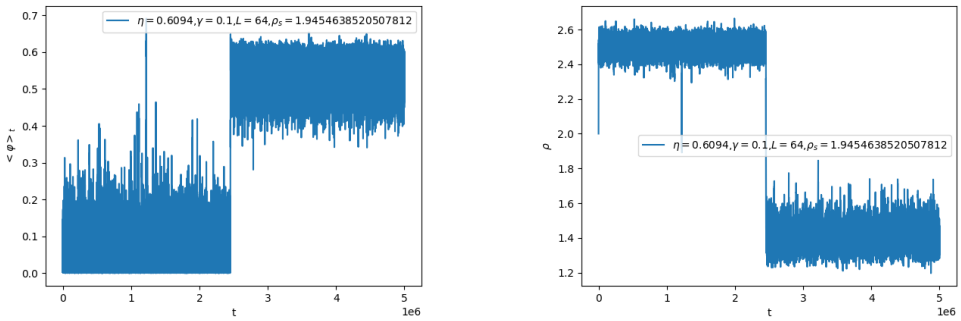

(a) (b)

Figure 27 – (a) Temporal evolution of the order parameter; (b) Temporal evolution of density. Parameters: $L = 64$, $\eta = 0.6094$, $\gamma = 0.1$ and $\nu = 100$.

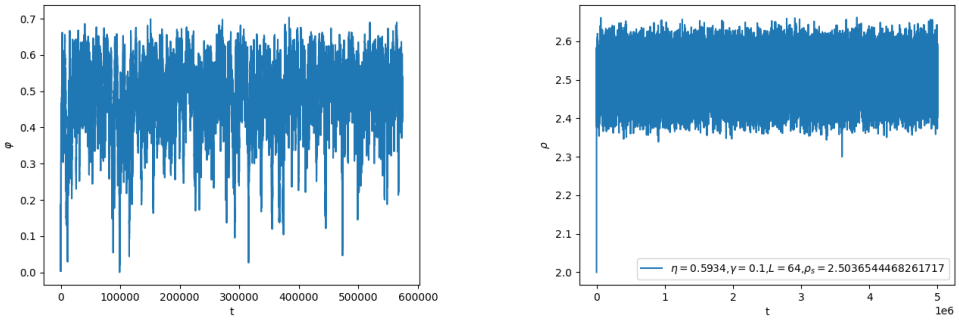

(a) (b)

Figure 28 – (a) Temporal evolution of the order parameter; (b) Temporal evolution of density. Parameters: $L = 64$, $\eta = 0.5922$, $\gamma = 0.1$ and $\nu = 20$.

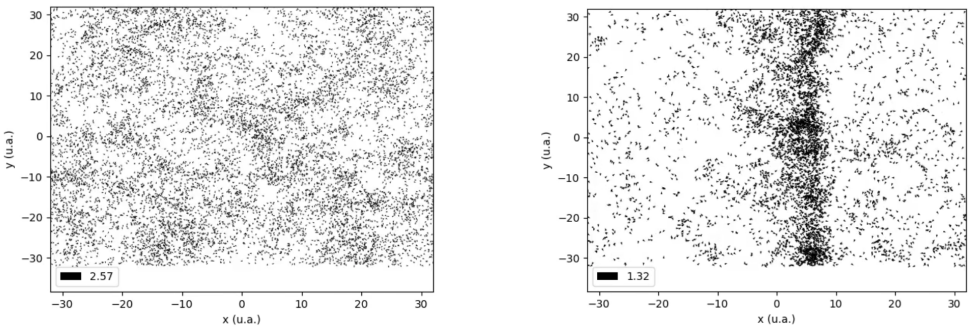

(a) (b)

Figure 29 – configurations for L = 64 and $\eta = 0.6094$. (a) t=1.5x 10^6; (b) t= 3.2x 10^6

To better understand the correlation between these two quantities, I calculate the Pearson coefficient between them. Pearson's correlation is given by:
corr $(\rho, \varphi) = \frac{C(\rho,\varphi)}{\sqrt{\sigma^2(\rho)\sigma^2(\varphi)}}$, where $C(\rho, \varphi)$ is the covariance of the order and density parameter, and $\sigma^2(\rho)$ and $\sigma^2(\varphi)$ represent the variance of the density and order parameter, respectively. Fig. 30 shows how Pearson's coefficient varies as a function of noise intensity.

We see from Fig. 30(b) that in the band regime there is a strong negative correlation between ρ and φ (Pearson correlation reaching -1). This is because when the order parameter is increased, bands form, causing a reduction in density. Since for $\nu = 20$ there are no bands, density and order parameter are only weakly correlated (Pearson correlation reaching -0.4).

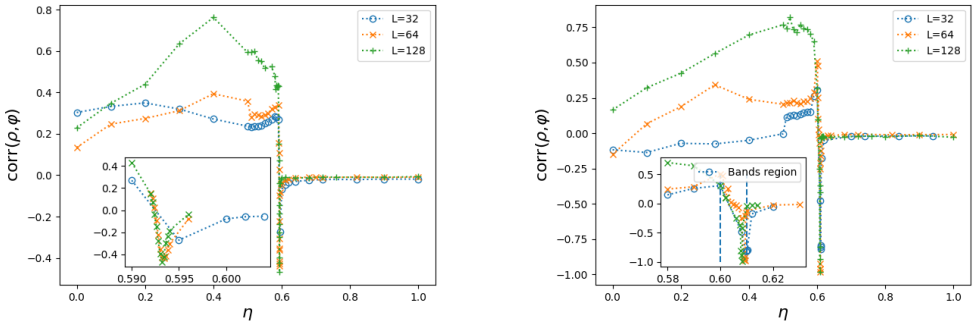

(a) (b)

Figure 30 – Pearson correlation coefficient $corr(\rho, \varphi)$ versus noise intensity for: $\gamma = 0.1$, $v_0 = 0.5$ and L as indicated. In (a) $\nu = 20$ and (b) $\nu = 100$.

In conclusion, our results points to a discontinuous phase transition for both $\nu = 20$ and $\nu = 100$. However, we observe bands only for $\nu = 100$. This suggests that the phase diagram for the VM with population dynamics is different for $\nu = 20$ and $\nu = 100$, as shown in Fig.31.

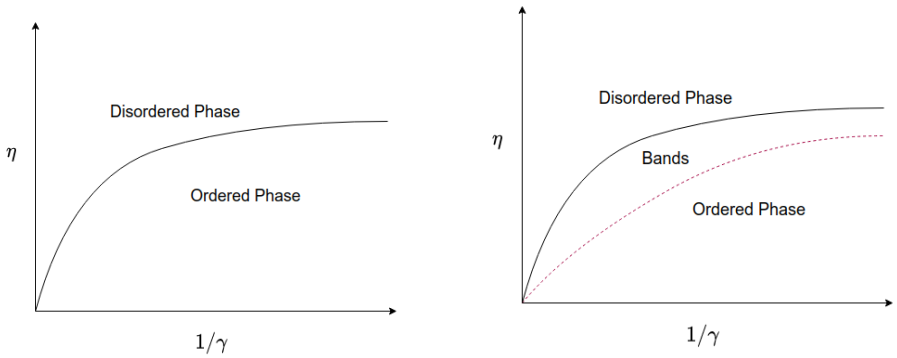

(a) (b)

Figure 31 – Qualitative phase diagram of Vicsek model with Malthusian dynamics for: (a) $\nu = 20$ and (b) $\nu = 100$.

5.5.3 Low-speed regime

We examine the effects of population dynamics on the low-speed regime. Fig. 32 shows the stationary density and the order parameter as a function of noise intensity.

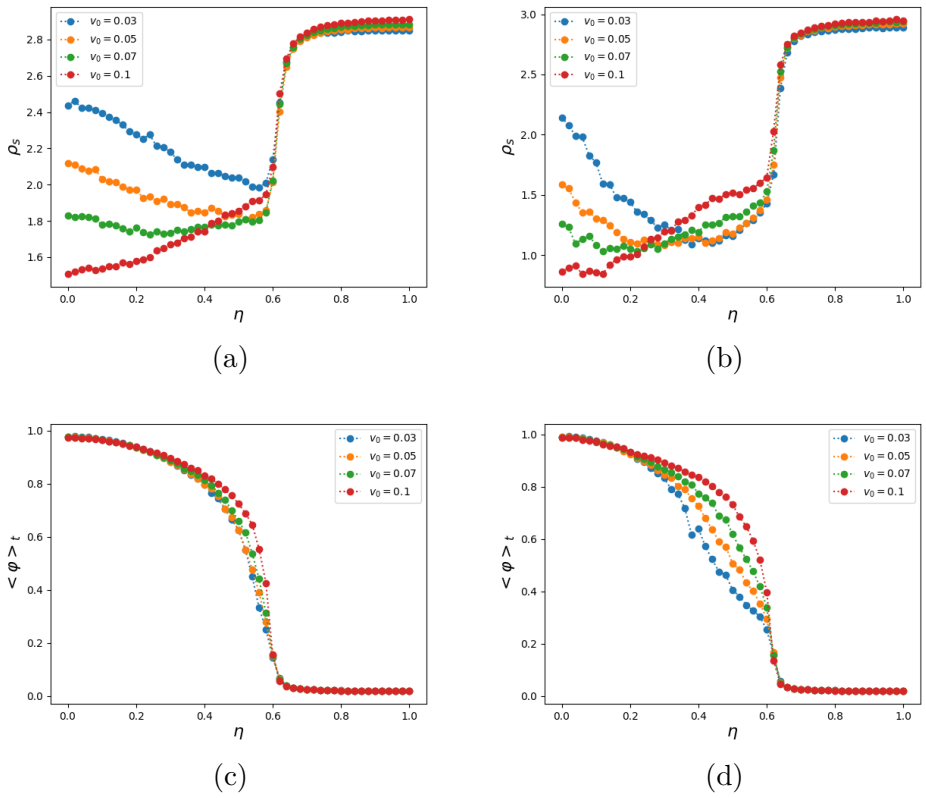

Figure 32 – Stationary density versus noise intensity for: $L = 32, \gamma = 0.1$ and velocity as indicated. In (a) $\nu = 20$ and in (b) $\nu = 100$.

Note in Fig. 32a and Fig. 32b that the stationary density decreases as the noise intensity increases for $v_0 = 0.03$ and $v_0 = 0.05$; the effect is weaker as we increase the speed. This seems to go against our earlier assertion that as noise intensity increases, density increases because particles become more evenly distributed. For extremely low velocities and $\eta \approx 0$, the particles travel in the same direction and but fill most of the available space, as shown in Fig. 33.

As we increase η, groups start to form and this leads to a lower density. Fig. 34 shows a typical snapshot in this regime. For lower velocities (Fig. 32a and 32a) the density has an unexpected behavior as we increase η. In section 5.5 we argued that the stationary density increases if we increase the intensity of noise η because for large values of η the particles spread better and this increases the density. However, we see in Fig. 32a and 32b a different behavior for low speeds. It turns out that for low speeds the formation of groups does not occur when the noise intensity is very small. Fig. 33 and 34 show just that. In Fig. 33 we have $\eta \simeq 0.0$, but the particles are more evenly distributed than in

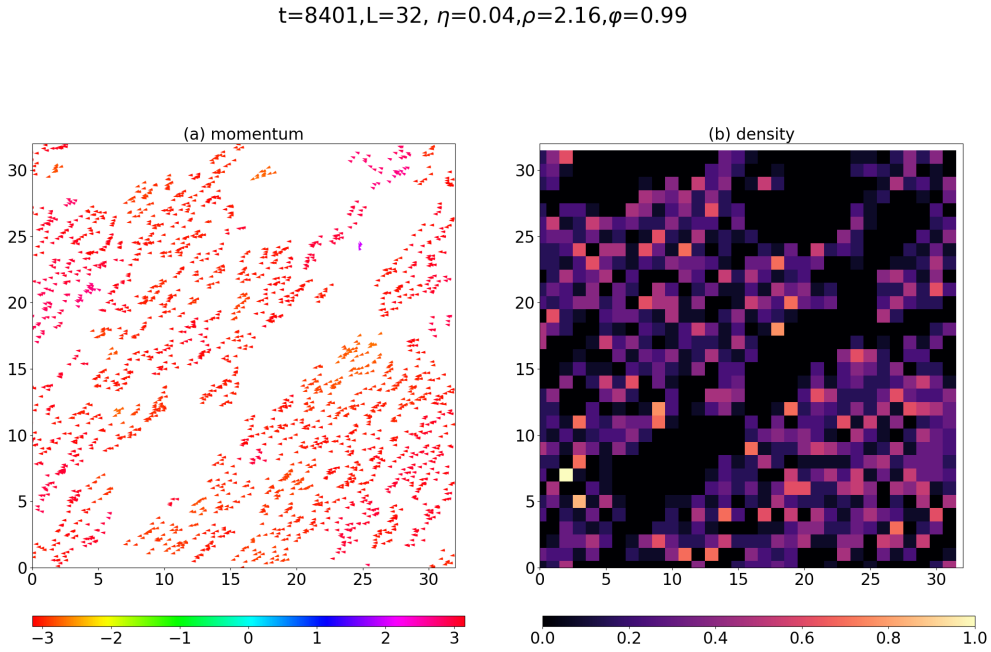

Figure 33 – Typical configuration for: $v_0 = 0.03, \eta = 0.04, L = 32, \gamma = 0.1$ and $\nu = 100$.

Fig.34, which has $\eta = 0.4$.

We still need a more deitaled study to undestand why particles in the low-velocity regime are evenly distributed for low noise intensities while this does not occur for particles with high velocity. One hypothesis is that when there are higher speeds, particles change neighborhoods more easily and this helps in the creation of groups.

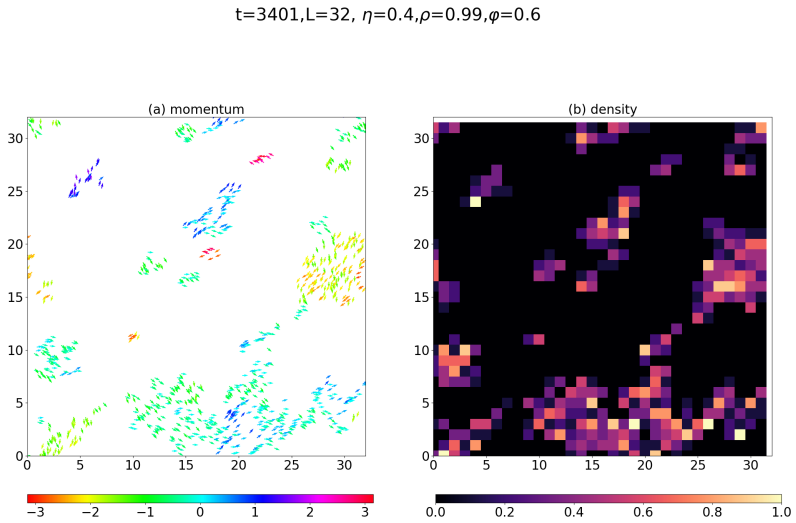

Figure 34 – Typical configuration for : $v_0 = 0.03, \eta = 0.4, L = 32, \gamma = 0.1$ and $\nu = 100$.

6 Conclusions and directions for future investigation

In this work, we studied a Vicsek model with population dynamics using computer simulations. Aiming to understand aspects that had not been studied theoretically in the Toner model [12], we construct a computational model of Monte Carlo where each self-propelled particle moves on its own, interacting with its neighbors, and the number of individuals varies as a result of a Malthusian population dynamics.

We obtained several interesting results, such as the fact that the formation of groups influences the stationary population density. We found a relation between noise and stationary density, and that orientational persistence decay more rapidly as we increase the rate of population dynamics.

The most surprising results are associated with the phase transition. We observe a discontinuous phase transition regardless of the rate, $1/\nu$, of the population dynamics.Nevertheless, the discontinuity weakens as we decrease ν. For example, hysteresis loop is smaller for $\nu = 10$ than for $\nu = 100$ (See section 17), ant the Binder cumulant attains more negative values for $\nu = 100$ than $\nu = 20$ (See section 5.5).

The coexistence regime of the Vicsek model is characterized by one or more dense ordered bands travelling through a disordered dilute region. The phase behavior for Vicsek model with slow population dynamics ($\nu = 100$) is rather similar to that of the original Vicsek model ($\nu = 100$). Under slow population dynamics, we observe coexistence, in the form of bands, of the ordered and disordered phases. For $\nu = 100$ there are, nevertheless, the following paradoxical tendencies: In the pure phases, both ordered and disordered, the density is an increasing function of the noise intensity, and thus a decreasing function of the degree of orientational order. The reason for this - increased noise leads to greater uniformity - is discussed in section 5.5. But, in the coexistence regime, it is the ordered phase that has the higher density.

For rapid population dynamics ($\nu = 20$) the phase transition continues to show signs of being discontinuous, in the behavior of the order parameter, the Binder cumulant, and the presence of hysteresis. Despite this, there is no sign of phase coexistence in the form of bands. The particle distribution is more uniform than for $\nu = 100$, though there are still significant deviations from a Poisson-distributed cell occupancy in the transition region, as reflected in $\tilde{p}$ (See Fig. 25).

In line with the preceding comment, further thought and analysis is necessary to understand how the transition remains discontinuous while signs of coexistence are

absent. A related question is whether, at some smaller, but finite value of ν, the transition turns continuous. It is also important to study the low-velocity regime, which exhibits a surprising behavior, in the formation of groups increases as we increase η in the weak noise regime (See section 5.5.3).

Our analysis of a Vicsek-like model including population dynamics was motivated by both theoretical and practical considerations, and appears to be the first study of its kind. Some of the results were unexpected, and required more detailed analyses to be understood; others remain as challenges for future work. Based on this experience, we have the impression that the study of active matter-experimentally, theoretically, and via simulation - still holds many surprises and opportunities for creative scientific investigation.

BIBLIOGRAPHY

[1] H. Chaté, F. Ginelli, G. Grégoire, and F. Raynaud. Collective motion of self-propelled particles interacting without cohesion. *Phys. Rev. E*, 77:046113, 2008. Citado 2 vezes nas páginas 19 and 33.

[2] A. Costanzo and C. K. Hemelrijk. Spontaneous emergence of milling (vortex state) in a vicsek-like model. *J. Phys. D: Appl. Phys.*, 51, 2018. Citado na página 12.

[3] O. Feinerman, I. Pinkoviezky, A. Gelblum, et al. The physics of cooperative transport in groups of ants. *Nature Phys*, 14:683–693, 2018. Citado na página 11.

[4] F. Ginelli. The physics of the vicsek model. *Eur. Phys. J. Spec. Top.*, 225:2099–2117, 2016. Citado 2 vezes nas páginas 21 and 28.

[5] G. Grégoire and H. Chaté. Onset of collective and cohesive motion. *Phys. Rev. Lett.*, 92:025702, 2004. Citado 6 vezes nas páginas 12, 13, 14, 17, 18, and 19.

[6] A. Gutierrez-Milla, F. Borges, R. Suppi, and E. Luque. Individual-oriented model crowd evacuations distributed simulation. *Procedia Computer Science*, 29:1600–1609, 2014. Citado na página 14.

[7] K. Kruse, J. Joanny, F. Jülicher, , and other. Generic theory of active polar gels: a paradigm for cytoskeletal dynamics. *Eur. Phys. J. E*, 16:5–16, 2005. Citado 3 vezes nas páginas 13, 22, and 24.

[8] T. R. Malthus. *An essay on the principle of population.* J. Johnson, St. Paul's Churchyard, London, 1798. Citado na página 22.

[9] W. Mather, O. Mondragón-Palomino, T. Danino, J. Hasty, and L. Tsimring. Streaming instability in growing cell populations. *Phys. Rev. Lett.*, 104:208101, 2010. Citado 3 vezes nas páginas 13, 22, and 24.

[10] Mermin and Wagner. Absence of ferromagnetism or antiferromagnetism in one- or two-dimensional isotropic heisenberg models. *Phys. Rev. Lett.*, 17:1133–1136, 1966. Citado 3 vezes nas páginas 12, 22, and 23.

[11] D. P. O'Brien. Analysis of the internal arrangement of individuals within crustacean aggregations (euphausiacea, mysidacea). *Journal of Experimental Marine Biology and Ecology*, 128(1):1–30, 1989. Citado na página 15.

[12] J. Toner. Birth, death, and flight: a theory of malthusian flocks. *Phys. Rev. Lett.*, 24, 2012. Citado 6 vezes nas páginas 12, 13, 22, 24, 25, and 46.

[13] J. Toner. Reanalysis of the hydrodynamic theory of fluid, polar-ordered flocks. *Phys. Rev. E*, 86:031918, 2012. Citado 4 vezes nas páginas 12, 22, 23, and 24.

[14] J. Toner and Y. Tu. Long-range order in a two-dimensional dynamical XY model: How birds fly together. *Phys. Rev. Lett.*, 75:4326–4329, 1995. Citado 3 vezes nas páginas 22, 23, and 24.

[15] S.-H. Tsai and S. R. Salinas. Fourth-order cumulants to characterize the phase transitions of a spin-1 ising model. *Brazilian Journal of Physics*, 28, 1998. Citado na página 53.

[16] Y. Tu, J. Toner, and M. Ulm. Sound waves and the absence of galilean invariance in flocks. *Phys. Rev. Lett.*, 80:4819–4822, 1998. Citado 3 vezes nas páginas 22, 23, and 24.

[17] T. Vicsek, A. Czirók, E. Ben-Jacob, I. Cohen, and O. Shochet. Novel type of phase transition in a system of self-driven particles. *Phys. Rev. Lett.*, 75:1226–1229, 1995. Citado 7 vezes nas páginas 11, 13, 14, 17, 18, 21, and 22.

Appendix

APPENDIX A – Discussion about the number of neighbors in vectorial noise

In this section we discuss in more detail how vectorial noise in VM depends on the number of neighbors. Suppose a particle with N neighbors. If we assume that the particle in question makes an error in evaluating the direction of each of these N particles and that these errors are independent, each coming from a particle, the total noise is:

$$\vec{S}_k = \sum_{i=1}^{N} \overrightarrow{\chi}_i, \tag{A.1}$$

where $\overrightarrow{\chi}_i$ is the noise added by particle i, given by a random vector of type:

$$\overrightarrow{\chi}_i = ke^{i\xi_i} = k[\mathbf{i}\cos\xi_i + \mathbf{j}\sin\xi_i], \tag{A.2}$$

where $< \xi_i >= 0$ and $< e^{\xi_k} e^{\xi_j} >= \delta_{kj}$. Clearly, $< S_k >= 0$ and we can calculate $< S_k^2 >$. So we have:

$$< |\vec{S}_k|^2 >= k^2 \sum_{i}^{N} [\cos^2\xi_i + \sin^2\xi_i] = Nk^2 \tag{A.3}$$

Hence the variance of noise with N independent contributions grows $\propto N$. However, if we write the vectorial noise as $\overrightarrow{\zeta} = N\eta e^{i\xi_i}$, we see that:

$$< |\overrightarrow{\zeta}|^2 >= N^2\eta^2[\cos^2\xi_i + \sin^2\xi_i] = N^2\eta^2 \tag{A.4}$$

Thus, the variance in vectorial noise grows $\propto N^2$. In this sense, we would have equivalence between the approaches using $\overrightarrow{\zeta}$ and $\vec{S}_k$ with $\overrightarrow{\zeta} \propto \sqrt{N}$.

APPENDIX B – Binder cumulant calculation

In this section we calculate the Binder cumulant for a vectorial order parameter with two components. Let the vectorial order parameter be given by:

$$\overrightarrow{\varphi} = \mathbf{i}\varphi_x + \mathbf{j}\varphi_y$$

.

Let's assume we are in the ordered phase, with the system moving in the direction **i**. Assuming that the parameter components are Gaussians, but in the **i** direction the mean is φ_0. Then we write the probability distributions for each as being:

$$\begin{aligned} p_1(\varphi_x) &= \frac{1}{\sqrt{2\pi}\sigma_1}\exp[-\frac{(\varphi_x-\varphi_0)^2}{2\sigma_1^2}] \\ p_2(\varphi_y) &= \frac{1}{\sqrt{2\pi}\sigma_2}\exp[-\frac{\varphi_y^2}{2\sigma_2^2}] \end{aligned} \tag{B.1}$$

To calculate the Binder cumulant we are interested in the second and fourth moments of φ. We can calculate them using:

$$< |\vec{\varphi}|^2 >=< (\hat{i}\varphi_x + \hat{j}\varphi_y)\cdot(\hat{i}\varphi_x + \hat{j}\varphi_y) >=< \varphi_x^2 + \varphi_y^2 >=< \varphi_x^2 > + < \varphi_y^2 > \tag{B.2}$$

These averages are easily calculated if we do:

$$< \varphi_x^2 >= \int_{-\infty}^{\infty} \varphi_x^2 p(\varphi_x)\, d\varphi_x \tag{B.3}$$

where $p(\varphi_x)$ is given by B.1. This integral is easy to calculate, and if we calculate $< \varphi_y^2 >$ similarly, we come to the conclusion that:

$$< \varphi^2 >= \varphi_0^2 + \sigma_1^2 + \sigma_2^2 \tag{B.4}$$

The fourth moment is giver for:

$$< \overrightarrow{\varphi}^4 >=< (\varphi_x^2 + \varphi_y^2)^2 >=< \varphi_x^4 > + < \varphi_y^4 > +2 < \varphi_x^2 >< \varphi_y^2 > \tag{B.5}$$

we already have the second moments of φ_x and φ_y, so we have to calculate their fourth moments that will be given by:

$$< \varphi_x^4 >= \int_{-\infty}^{\infty} \varphi_x^4 p(\varphi_x)\, d\varphi_x \tag{B.6}$$

and similarly for φ_y.

This integral is easily calculated and we find that:

$$< \varphi^4 >= 3(\sigma_1^4 + \sigma_2^4) + \varphi_0^4 + (2\sigma_2^2 + 6\sigma_1^2)\varphi_0^2 + 2\sigma_1^2\sigma_2^2 \tag{B.7}$$

Now we calculate the Binder cumulant:

$$G = 1 - \frac{1}{3}\frac{< \varphi^4 >}{< \varphi^2 >^2} = 1 - \frac{1}{3}\frac{3(\sigma_1^4 + \sigma_2^4) + \varphi_0^4 + (2\sigma_2^2 + 6\sigma_1^2)\varphi_0^2 + 2\sigma_1^2\sigma_2^2}{\varphi_0^4 + \sigma_1^4 + \sigma_2^4 + 2\sigma_1^2\sigma_2^2 + 2(\sigma_2^2 + \sigma_1^2)\varphi_0^2} \tag{B.8}$$

For the disordered phase $\varphi_0 \to 0$ and $\sigma_1 = \sigma_2 = \sigma$. Hence, $G \approx 1/3$.
In the ordered phase, σ_1 and $\sigma_2 \to 0$ and $G \approx 2/3$. Now consider the coexistence of ordered and disordered phases, in the proportions λ and $1 - \lambda$. It is easy to show that in this case the variation of G, varying λ in the interval [0,1], is non-monotonic, and that G can take negative values depending on the ratio σ/φ_0 [15].

APPENDIX C – Monte Carlo

In order to know the properties of a thermodynamic system we need the probability distribution $P(X_t)$, where X_t are the possible states of the system. Any average can be obtained from $P(X_t)$ through:

$$< f >= \sum_{X_t} f(X_t)P(X_t), \tag{C.1}$$

where we sum over all particles.

The Monte Carlo method gives an average of f using the following: Suppose we generate N states according to the probability $P(X_t)$. We can then calculate the average of f, which will be given for:

$$< f >= \frac{1}{N}\sum_{i=1}^{N} f(X_i), \tag{C.2}$$

with X_1,X_2,...,X_N being the states generated in the process.

The question that remains now is: How to build a chain whose stationary distribution corresponds to the distribution of states? Since we are working out of equilibrium, we do not know the probability distribution of states. What we do then is generate a random initial state and let the system evolve in time, and when the system reaches its steady state, we apply the formula C.2 in which, the more states are generated, the better our average $< f >$.

APPENDIX D – Algorithm of simulation

Algorithm 2 Complete algorithm of Vicsek model with population dynamics

Assign a random position to each particle in the system of size L
Assign a random θ to each particle in the interval $[-\pi, \pi]$
for $t < t_{\text{maximum}}$ **do**
    Assign to each particle it's cell
    Create a list with every particle that are in a cell
    for i=1,N$_{vivas}$ **do** ▷ Loop over all particles
        for j **do** ▷ Loop over all particle in the cell of particle i and neighbor cells
            Verify if i and j are neighbors ▷ Condition: $d = \sqrt{r_i^2 + r_j^2} \leq 1$
        end for
        Calculate the mean θ between i and it's neighbors ▷ attention to the type of noise
        Add up the noise
        Save the new θ of particle i
    end for
    Update the θ and position of each particle
    ▷ POPULATION DYNAMICS
    $m_e = N_{vivas}/\nu$ ▷ The mean number from the Poisson distribution
    $n_e = \text{ignpoi}(m_e)$ ▷ The number of particles that will participate in the population dynamics
    for i=1,n_e **do**
        Choose randomly a particle i
        Calculate p_i^d
        Chose randomly a number in the interval $[0, 1]$
        if $r \leq p_i^d$ **then**
            Particle i dies
        else
            A particle is created
            Assign a position to the new particle ▷ See eq.3.8
            Assign a random θ to new particle in the interval $[-\pi, \pi]$
        end if
    end for

APPENDIX E – Simulation code in FORTRAN90

```
program New_vicsek
!CONSTRUÇÃO DAS CÉLULAS: M.P.Allen.D.J. Tildesley-Computer Simulation of liquids- Chapter 5
    implicit none
    character(len=5)::nomej,nomecell
    character(len=6):: nomep
    character(len=4)::nomek
    character(len=3)::nomeL
    real::p_e,rand
    integer,parameter::tmax=10000,trel=0
    complex,parameter::im=(0,1)
    real(kind=4),dimension(2)::vec_phi
    integer,external::ignpoi !chamar a variavel de uma distribuição de poisson de média dada
    real(kind=4),parameter::Lx=25.0,Ly=25.0,Lx2=Lx/2,Ly2=Ly/2,rLx=1/Lx,rLy=1/Ly,pi=3.14159265
    real(kind=4),parameter::dois_pi=2*pi,e=2.71828182845904523536028 7
    integer,parameter::scx=int(Lx),scx1=scx-1,scy=int(Ly),scy1=scy-1,div_H=10,div_H_1=div_H-1
    integer,parameter::ninit=300,nmax=301
    real(kind=4),dimension(nmax)::x,y,teta,sen_m,cos_m,vx,vy,gteta
    real(kind=4)::r_cut,r_viz,dx,dy,v0,dist
    real(kind=4)::sum_vx,sum_vy,tetamed,order_par,order_par_med,noise,eta
    real(kind=4)::gama,pd,dens_media,dens,par_o,gamnumviz
    integer::nvivas,nmortas,n_med,nu,num_e
    integer,dimension(2,nmax)::k,K_H !celula de uma particula
    integer,dimension(0:scx1,0:scy1)::head,n_H,nxy!head aponta qual a primeira particula na celula e n é o
                                                  !numero de part na celula
    integer(kind=4),dimension(nmax)::link,vivas,mortas,num_viz!1link aponta a proxima (link(i)=0
                                                             !acabou a contagem),
                                                            !vivas e mortas dizem quais tao vivas ou não
    integer::t,j,m1,p,i,inew,i1,mnew,gnew,m,g,num_viz_din,numb,part
    integer::cont3,born,nvivasd,cont_pos
    integer::cont_H,cont5,cont_viz,cont_cell
    complex::z
    real::r,xsi,psi,phi
    call random_seed()
    !==VARIAVEIS INICIAIS=======================
    p=4
    gama=0.100
    nu=100
    m1=155
    eta=0.0100*float(m1)
    v0=0.03
    r_cut=1.0
    r_viz=1.0
    !====================ARQUIVOS============================
    write(*,*)eta,dens_media
    write(nomeL,'(I3.3)')scx
    write(nomek,'(I4.4)')m1
    write (nomep, '(f6.3)')gama
    open(unit=1,file='./info'//nomek//'.dat',status='unknown',action='write')
    open(unit=2, file='./kuramoto'//nomek//'.dat', status='unknown', action='write') !GUARDA AS VARIAVEIS DE
                                                                                     ! KURAMOTO DO SISTEMA
    open(unit=7, file='dados_H'//nomek//'.dat', status='unknown', action='write')!GUARDA O NÚMERO DE
                                                                                !PARTICULAS NUMA CELULA DE TAMANHO 0.1*L
    open(unit=10, file='p_e'//nomek//'.dat',status='unknown',action='write') !MONITORA P_E E OUTRAS VARIAVEIS
    open(unit=11, file='nvivas'//nomek//'.dat',status='unknown',action='write') !GUARDA NVIVAS PARA AS CELULAS
```

```
55      cont5=cont_pos-1
56      cont_viz=0
57      cont_cell=0
58
59      write(1,*)Lx
60      write(1,*)v0
61      write(1,*)r_cut
62      write(1,*)r_viz
63      write(1,*)eta
64      write(1,*)m1
65      write(1,*)gama
66      write(1,*)cont_pos
67      write(1,*)tmax
68      close(1)
69
70      n_med=0
71
72
73      !-------CONDIÇÕES INICIAIS-----------------------
74      nvivas=ninit
75      nmortas=nmax-ninit
76
77      !---CRIANDO VIVAS/MORTAS-------------
78      do i=1,nmax
79      if (i.le.ninit) then
80      vivas(i)=i !no inicio crio o vetor de vivas indo de 1,...,nvivas,0,0,0,0... até nmax
81      else
82      vivas(i)=0
83      end if
84      end do
85      do i=1,nmax
86      if (i.le.nmortas) then
87      mortas(i)=i+ninit
88      else
89      mortas(i)=0
90      end if
91      end do
92      !-------------------------------------
93
94      do i=1,nvivas !distribuição aleatoria inicialmente
95      call random_number(rand)
96      x(vivas(i))=(rand-0.5)*Lx
97      call random_number(rand)
98      y(vivas(i))=(rand-0.5)*Ly
99      call random_number(rand)
100     teta(vivas(i))=dois_pi*(rand-0.5)
101     end do
102
103     order_par=0.00
104     vec_phi(:)=0.0
105
106     do t=1,tmax
107     !=============ZERANDO AS VARIAVEIS=================
108
```

```
109     dens=float(nvivas)/(Lx*Ly)
110
111     z=(0.0,0.0)
112     sum_vx=0.00
113     sum_vy=0.00
114
115     !===========COLOCAR AS PARTICULAS EM CÉLULAS============
116     head(:,:)=0
117     nxy(:,:)=0
118     do i1=1,nvivas
119     k(1,vivas(i1))=((x(vivas(i1))+Lx2)*rLx)*scx
120     if (x(vivas(i1)).ge. (Lx2-0.0001)) then !antierro
121     k(1,vivas(i1))=scx1
122     end if
123     if (k(1,vivas(i1)).gt. scx1 .or. k(1,vivas(i1)).lt. 0) then
124     write(*,*)'erro k1', x(vivas(i1)),y(vivas(i1))
125     goto 70
126     end if
127     k(2,vivas(i1))=((y(vivas(i1))+Ly2)*rLy)*scy
128      if (y(vivas(i1)).ge. (Lx2-0.0001)) then !antierro
129     k(2,vivas(i1))=scy1
130     end if
131     if (k(2,vivas(i1)).gt. scy1 .or. k(2,vivas(i1)).lt. 0) then
132     write(*,*)'erro k2', x(vivas(i1)),y(vivas(i1))
133     goto 70
134     end if
135     nxy(k(1,vivas(i1)),k(2,vivas(i1)))=nxy(k(1,vivas(i1)),k(2,vivas(i1))) + 1
136     link(vivas(i1))=head(k(1,vivas(i1)),k(2,vivas(i1)))
137     head(k(1,vivas(i1)),k(2,vivas(i1)))=vivas(i1)
138     end do !i1
139     if (sum(nxy).ne.nvivas)then
140         write(*,*) 'sum(nxy) =/ nvivas'
141         goto 70
142     end if
143
144     !=========GUARDANDO O NUMERO DE PARTICULAS EM CELLS 1X1============
145     if (t .gt. int(0.8*tmax)) then
146         cont3=cont3+1
147         if (cont3==1000) then
148          cont_cell=cont_cell+1
149          write (nomecell, '(I5.5)')cont_cell
150          open(9,file='./cell'//nomecell//'.dat',action='write')
151          do i=0,scx1
152             do j=0,scy1
153                 write(9,*) nxy(i,j)
154             end do
155          end do
156          close(9)
157          cont3=0
158         end if
159     end if
160
161 !========GUARDANDO O NUMERO DE PARTICULAS EM CELLS 0.1L======================
162   ! if (t.gt. int(0.8*tmax)) then
```

```
!       n_H(:,:)=0
!       do i=1,nvivas
!         k_H(1,vivas(i))=int(((x(vivas(i))+Lx2)*rLx)*div_H)
!         k_H(2,vivas(i))=int(((y(vivas(i))+Ly2)*rLy)*div_H)
!         n_H(k_H(1,vivas(i)),k_H(2,vivas(i)))=n_H(k_H(1,vivas(i)),k_H(2,vivas(i)))+1
! end do
!do i=0,div_H_1
!         do j=0,div_H_1
!         write(7,*) n_H(i,j)
!         end do
!end do
!cont_H=0
!       end if
!  end if
  !====================ALINHAMENTO DAS PARTICULAS==========================
  do i=1,nvivas
      gteta(vivas(i))=teta(vivas(i)) !guarda o teta antigo para a dinâmica enquanto teta vai sen
  end do
  do i=1,nvivas
  num_viz(vivas(i))=0
  inew=vivas(i)
  sen_m(inew)=0.0
  cos_m(inew)=0.0
  do m=k(1,inew)-1,k(1,inew)+1
  do g=k(2,inew)-1,k(2,inew)+1
  mnew=m
  gnew=g
  !==========CONDIÇÕES DE CONTORNO==============================

      if (mnew.lt.0) then
      mnew=mnew+scx
      else if (mnew.gt.scx1) then
      mnew=mnew-scx
      end if

      if (gnew.lt.0) then
      gnew=gnew+scy
      else if(gnew.gt.scy1) then
      gnew=gnew-scy
      end if
  !=====================================================================
  j=head(mnew,gnew)
  do
  if (j==0) then
  goto 10
  end if
  !----------------------------------------
  dx=abs(x(inew)-x(j))
  if (dx.gt.Lx2) then
  dx=Lx-dx
  end if
  dy=abs(y(inew)-y(j))
  if (dy.gt.Ly2) then
  dy=Ly-dy
```

```
219     end if
220     dist=sqrt(dx*dx+dy*dy)
221     if (dist.le.r_cut) then
222     num_viz(vivas(i))=num_viz(vivas(i))+1
223     sen_m(inew)=sen_m(inew)+sin(gteta(j))
224     cos_m(inew)=cos_m(inew)+cos(gteta(j))
225     end if
226     j=link(j)
227     end do !j
228     10  continue
229     end do !m
230     end do !g
231     call random_number(rand)
232     noise=dois_pi*(rand-0.5)
233     !sen_m(inew)=sen_m(inew) + float(num_viz(vivas(i)))*eta*sin(noise) !ruído vetorial
234     !cos_m(inew)=cos_m(inew) + float(num_viz(vivas(i)))*eta*cos(noise) !ruído vetorial
235     teta(inew)=atan2(sen_m(inew),cos_m(inew)) + eta*noise !ruído angular
236     vx(inew)=v0*cos(teta(inew)) !ATUALIZAR VELOCIDADES
237     vy(inew)=v0*sin(teta(inew))
238
239     !--------mantendo teta entre -pi,pi--------------------------
240     if (teta(inew).lt.(-pi)) then
241     teta(inew)=teta(inew)+ dois_pi
242     end if
243     if (teta(inew).gt.pi) then
244     teta(inew)=teta(inew)- dois_pi
245     end if
246     end do !i
247     !======================VIZINHOS=======================================
248     cont5=cont5+1
249     if(cont5==cont_pos) then
250     cont_viz=cont_viz+1
251     write (nomej, '(I5.5)')cont_viz
252     open(3,file='./position'//nomej//'.dat',action='write')
253     open(8,file='./vizinhos'//nomej//'.dat',action='write')
254     write(11,*)nvivas
255     do i=1,nvivas
256     write(8,*)vivas(i),x(vivas(i)),y(vivas(i)),num_viz(vivas(i))
257     write(3,*)x(vivas(i)),y(vivas(i)),cos(teta(vivas(i))),sin(teta(vivas(i)))
258     end do
259     close(8)
260     close(3)
261     cont5=0
262     end if
263     !=======================================ATUALIZAR POSIÇÕES=========================
264     do i=1,nvivas
265     inew=vivas(i)
266     x(inew)=x(inew)+vx(inew)
267     y(inew)=y(inew)+vy(inew)
268     x(inew)=x(inew)-nint(x(inew)*rLx)*Lx
269     y(inew)=y(inew)-nint(y(inew)*rLy)*Ly
270     !-------------ANTI ERRO-----------------------------------/
271     if(x(inew).gt.(Lx2) .or. y(inew).gt.(Ly2))then
272     write(*,*)x(i1),y(i1),'celulas'
```

```
273     write(*,*) 'fora dos limites'
274     goto 70
275     end if
276     if (x(inew).lt.(-Lx2) .or. y(inew).lt.(-Ly2)) then
277     write(*,*)x(inew),y(inew),'celulas'
278     write(*,*) 'fora dos limites'
279     goto 70
280     end if
281     !-------------------------------------------------------------
282     end do
283     do i=1,nvivas
284     sum_vx=sum_vx+vx(vivas(i))
285     sum_vy=sum_vy+vy(vivas(i))
286     end do
287     vec_phi(1)=sum_vx/(nvivas*v0)
288     vec_phi(2)=sum_vy/(nvivas*v0)
289     par_o=sqrt(vec_phi(1)**2+vec_phi(2)**2)
290     order_par = order_par + sqrt(sum_vx*sum_vx + sum_vy*sum_vy)/(V0*nvivas)
291     order_par_med=order_par/t
292     write(15,*)t,dens,par_o
293
294
295      !===============DINAMICA POPULACIONAL=================================
296     if (t.gt.1e8) then
297     nvivasd=nvivas
298     p_e=float(nvivas)/float(nu)
299     num_e=ignpoi(p_e)
300     write(10,*)p_e,nvivas,num_e,dens
301     do i=1,num_e
302     call random_number(rand)
303     numb=int((rand*nvivasd)+1)
304     part=vivas(numb)
305     num_viz_din=0
306     gamnumviz = gama*float(num_viz(part))
307     pd=gamnumviz/(gamnumviz+1)
308     call random_number(rand)
309     if (rand.le. pd) then !UMA PARTICULA MORRE
310     nvivasd=nvivasd-1
311     nmortas=nmortas+1
312     mortas(nmortas)=part !se a particula morreu ela passa a ser a ultima do vetor mortas
313     vivas(numb)=vivas(nvivas)!e sua posição em vivas é trocada pela a ultima que tinhamos
314     nvivas=nvivas-1
315     else !uma particula nasce. part vai ser a "mãe" !numb2 está entre [1,nmortas]
316     !colocar um if aqui
317     born=mortas(1) !essa part vai nascer
318     nvivas=nvivas+1
319     vivas(nvivas)=born
320     mortas(1)=mortas(nmortas)
321     nmortas=nmortas-1
322     if (nvivas.eq.0) then
323     write(*,*) ' nvivas=0'
324     goto 70
325     end if
326     !ABAIXO ESTÁ ONDE VAI NASCER A NOVA PARTÍCULA
```

```
327     call random_number(rand)
328     x(vivas(nvivas))=x(part) + 0.5*rand
329     call random_number(rand)
330     y(vivas(nvivas))=y(part) + 0.5*rand
331     call random_number(rand)
332     teta(vivas(nvivas))=dois_pi*(rand-0.5)
333     x(vivas(nvivas))=x(vivas(nvivas)) - (nint(x(vivas(nvivas))*rLx))*Lx
334     y(vivas(nvivas))=y(vivas(nvivas)) - (nint(y(vivas(nvivas))*rLy))*Ly
335     !======================VARIAVEIS DE KURAMOTO====================
336
337     if(nvivas.ge.nmax) then
338     write(*,*)nvivas,'nvivas maior que nmax'
339     goto 70
340     end if
341     end if
342     end do
343     end if
344  !======================FIM DA DINÂMICA POPULACIONAL=====================================
345
346     do i=1,nvivas
347     z=z+e**(im*teta(vivas(i)))
348     end do
349     z=z/nvivas
350     psi=real(z)
351     xsi=imag(z)
352     phi = atan2(xsi,psi)
353     r=sqrt(psi**2+xsi**2)
354     !write(2,*) t,phi,psi,xsi,r
355     if(t.gt. int(0.9*tmax)) then
356     n_med=n_med+nvivas
357     end if
358     end do !t
359     70  continue
360     close(2)
361     close(5)
362     close(7)
363     close(10)
364     close(11)
365     close(15)
366 end program
```